8-2020

Study of Levee Underseepage through Abandoned Channels and Point Bars on Curved Levee Sections Using the Response Surface-Monte Carlo Method

Tomsen Reed
Utah State University

STUDY OF LEVEE UNDERSEEPAGE THROUGH ABANDONED CHANNELS AND POINT BARS ON CURVED LEVEE SECTIONS USING THE RESPONSE SURFACE-MONTE CARLO METHOD

by

Tomsen Reed

A thesis proposal submitted in partial fulfillment
of the requirements for the degree

of

MASTER OF SCIENCE

In

Civil and Environmental Engineering

Approved:

_____	_____
John Rice, Ph.D. Major Professor	James Bay, Ph.D. Committee Member
_____	_____
Tom Lachmar, Ph.D. Committee Member	Janis L. Boettinger, Ph.D. Acting Vice Provost of Graduate Studies

UTAH STATE UNIVERSITY
Logan, Utah

2020

ABSTRACT

Study of Levee Underseepage through Abandoned Channels and Point Bars on Curved Levee Sections Using the Response Surface-Monte Carlo Method

by

Tomsen Reed, Master of Science

Utah State University, 2020

Major Professor: Dr. John Rice
Department: Civil and Environmental Engineering

Underseepage can lead to levee failure, typically as a result of one of two conditions: 1) backward erosion piping, or 2) heave. Levees create a condition of head differential, where the head on the riverside of the levee is significantly higher than that on the landside which leads to underseepage through the foundation layer. This can cause heave (uplift and cracking) of the blanket layer if the uplift pressure is high enough, or it can also lead to backward erosion piping if the hydraulic gradient through the foundation material is high enough. Both the pressure and gradient are results of the head of the water at a given point on the landside of the levee.

One of the most widely used levee design methods is the Blanket Theory method, which assumes a simple landside soil profile of a layer of low permeability material underlain by a foundation material of higher permeability. This theory assumes that these strata are deposited horizontally and have a constant thickness. Failure has occurred

where the strata are not completely horizontal and where geomorphic features interrupt layers and allow head to concentrate.

Geomorphic features that occur in the fluvial deposits often associated with levees include the crevasse splay, abandoned channels, point bars and meander scrolls. The research herein focused on point bars and meander scrolls, two related geomorphic features that are formed as a river migrates and deposits mostly granular material on one bank. The existence of a point bar underlying a levee can pose a serious problem that is often overlooked by Blanket Theory equations. This research created a model of point bar behavior (or a response surface) to be integrated with research by Dr. John Rice and Lourdes Polanco that uses a Monte Carlo simulation to perform a reliability analysis of levees that are possibly underlain by point bars and abandoned channels. The initial three-dimensional finite-element model was created using a program called SVFlux, by SoilVision (SoilVision, 2014). The use of this method allows for a more accurate depiction of the risk involved in constructing a levee with uncertain foundation characteristics.

(103 pages)

PUBLIC ABSTRACT

Study of Levee Underseepage through Abandoned Channels and Point Bars on Curved Levee Sections Using the Response Surface-Monte Carlo Method

Tomsen Reed

The current procedures for calculated the probability of failure of levees (earthen structures designed to prevent flooding of important locations) all have their own unique limitations. Some methods are very simplistic, and either ignore or do not allow for inclusion of complex geometries. Other methods allow for complex geometry, but do not lend themselves to large quantities of analysis because of the amount of time it takes to create or modify a model. For these reasons, previous research performed by Lourdes Polanco and Dr. John Rice developed the preliminary stages of a new method called the Response Surface-Monte Carlo method. This method not only accounts for complex geometry, it is a probabilistic method that has the ability to calculate the probability of erosion initiation within a levee section. The research contained herein focused on a specific aspect of Dr. Rice's work on levees which involved the creation of a "response surface" or a type of model for curved levees and for levees overlying a specific riverside feature known as a point bar. A point bar is a river feature that can, if it underlies a levee, potentially decrease the performance thereof.

ACKNOWLEDGMENTS

I would like to first of all thank my wife for the encouragement and support she has given me throughout this process of finishing my degree. I really am so grateful to for everything she has done for me and for our family. I would also like to thank my advisor, Dr. John Rice for the patience he has had with me throughout this process of research and writing, and for all of his advice and counsel. Dr. Jim Bay, Dr. Tom Lachmar, and Lourdes Polanco Boulware were also great supports and resources, and I'm also grateful to them.

CONTENTS

Page

ABSTRACT iii
PUBLIC ABSTRACT v
ACKNOWLEDGMENTS vi
LIST OF TABLES ix
LIST OF FIGURES xi
INTRODUCTION 1
Summary 1
Purpose 2
Significance 3
Organization 3
LITERATURE REVIEWED 5
Current Levee Underseepage Analysis Methods 5
Response Surface-Monte Carlo Method 7
Effects of Levee Curvature 8
River/Point Bar Geomorphology 10
METHODOLOGY 16
Problem Statement 16
Overview of Methodology 18
Response Surface Methodology 19
ANALYSIS OF DATA 23
Data Collected 23
Parametric Analysis 29
Summary of Behavior 48
Response Surface for a Straight Levee 51
Effects of Levee Curvature 54
Curvature Multiplier 56
CONCLUSION 73

REFERENCES 77

APPENDICES 80

APPENDIX A 81

APPENDIX B 88

LIST OF TABLES

Table Page

1 Results from experimenting with the “l” and “L” parameters while maintaining a constant ratio of the two 44

2 Experimentation with the two geometric parameters "l" and "L", maintaining "l" constant and changing the ratio of the two 46

3 Experimentation with the "l" parameter, changing it while keeping "L" constant 46

4 Effects of having an entirely curved levee section vs. partially curved and partially straight levee section 47

5 Parameters and results for the curvature model with Dc = 90º and α = 90º 59

6 Parameters and results for the curvature model with Dc = 90º and α = 45º 62

7 Parameters and results for the curvature model with Dc = 150º and α = 90º 64

8 Parameters and results for the curvature model with Dc = 150º and α = 45º 66

9 Parameters and results for the curvature model with Dc = 60º and α = 90º 69

10 Parameters and results for the curvature model with Dc = 60º and α = 45º 71

A-1 Fit-equations’ coefficients and corresponding goodness of fit for family of curves with respect to each λm used 86

B-1 Parameters and normalized results for the curvature model with Dc = 60º and no point bar, to compare with results from Benjasupattananan (2013). ND = arc-length normalized distance from center of curvature. Head measured at landside levee toe and normalized to values calculated on linear sections distant from curved section. 88

B-2 Parameters and results for the curvature model with Dc = 90º and no point bar, to compare with results from Benjasupattananan (2013). ND = arc-length normalized distance from center of curvature. Head measured at landside levee toe and normalized to values calculated on linear sections distant from curved section. 89

B-3 Parameters and results for the curvature model with Dc = 150º and no point bar, to compare with results from Benjasupattananan (2013). ND = arc-length normalized distance from center of curvature. Head measured at landside levee toe and normalized to values calculated on linear sections distant from curved section. 89

LIST OF FIGURES

Figure		Page
1	Effect of levee curvature on pressure head	9
2	Graphic of several geomorphic features, modified from Allen (1970)	11
3	Cross-sectional depiction of water flow and point bar initiation in alluvial rivers, from Nanson (1980)	12
4	"Ridge and swale" topography characteristic of meander scrolls, from Woolfe and Purdon (1996)	13
5	Photograph of the topography above a meander scroll, from Woolfe and Purdon (1996)	14
6	Depiction of clay "drapes" that accumulate in between subsequent point bars to create a meander scroll, from Gagliano and Van Beek (1970, published in Saucier 1994)	15
7	Convention for radial distance, modified from William Lettis and Associates (2008).	24
8	Map created by William Lettis and Associates (2008) outlining the locations of point bars and meander scrolls in the Sacramento area	26
9	Top and side views of the geometry of the point bar and levee alignment, not to scale	28
10	Two-dimensional model of the longitudinal representation of the point bar	29
11	Two-dimensional model of the transverse representation of the point bar	29
12	A representation from SVFlux of how the point bar was shortened in this section of the experiment	33
13	Plot showing the effect of the point bar length on hydraulic head at landside levee toe	34
14	Angle of incidence vs. hydraulic head at landside levee toe	35

Figure Page

15 From SVFlux, showing the convention for measuring the angle (in degrees) of entry of the point bar. The shape in between the gray lines represents the point bar 35

16 Hydraulic gradient vs. permeability ratio of point bar to blanket, with a blanket permeability of 1 x 10-7 feet/second 36

17 Representations from SVFlux of the degrees of curvature. The yellow region represents the point bar 37

18 A chart showing the effect of the radius vs. the head calculated in the middle of the point bar 38

19 A graph showing the effect of the radius on the head calculated in the point bar directly below the landside levee toe 39

20 The head calculated in each point bar at the landside levee toe in the case of several point bars within one levee alignment (a meander scroll) with a radius of 1300 feet and 180 degrees of curvature 40

21 The head calculated in each point bar at the landside levee toe in the case of several point bars within one levee alignment (a meander scroll) with a radius of 1300 feet and 30 degrees of curvature 41

22 The head calculated in each point bar at the landside levee toe in the case of several point bars within one levee alignment (a meander scroll) with a radius of 1300 feet and 90 degrees of curvature 41

23 The head calculated in each point bar at the landside levee toe in the case of several point bars within one levee alignment (a meander scroll) with a radius of 800 feet and 180 degrees of curvature 42

24 A comparison of the head calculated at the landside levee toe in an alignment with three point bars, changing the thickness of the clay "drape" in between each subsequent point bar 43

25 Representations showing the "l" parameter, as well as the "L" parameter, two geometric parameters that relate the point bar to the levee alignment 44

Figure Page

26 Comparison of a completely curved levee section to a levee section with a portion curved and two straight levee sections on either side 47

27 A view of the “tongue effect” mesh and head contours generated by SVFlux within a levee with 180 degrees of curvature 50

28 Angle of incidence, α, for two point bars crossing a levee section, with values of α=45° and α=90° 52

29 Effect of levee curvature on pressure head, from Benjasupattananan (2013) ... 55

30 Schematic plan view of the curvature model used for Dc = 60º and α = 90º showing channel features at ND = -5, -1, +3, +7 55

31 Graph depicting the effect of curvature on head at the toe of a levee, with and without a point bar underneath. Dc = 60º and α = 90º, λm = 83.7, Tch =1 56

32 Schematic plan view of the curvature model used for Dc = 90º and α = 90º showing point bar features at ND = -4, 0, +1 +3 57

33 Results for the curvature model with Dc = 90º and α = 90º 58

34 Schematic plan view of the curvature model used for Dc = 90º and α = 45º showing point bar features at ND = -4, 0, +1 +3 60

35 Results for the curvature model with Dc = 90º and α = 45º 61

36 Results for the curvature model with Dc = 150º and α = 90º 63

37 Schematic plan view of the curvature model used for Dc = 150º and α = 90º showing point bar features at ND = -3, -1, 0 +2 63

38 Schematic plan view of the curvature model used for Dc = 150º and α = 45º showing channel features at ND = -3, -1, 0, +2 65

39 Results for the curvature model with Dc = 150º and α = 45º 67

40 Results for the curvature model with Dc = 60º and α = 90º 67

Figure Page

41 Schematic top view of the curvature model used for Dc = 60º and α = 45º showing channel features at ND = -5, -2, +3, +5 70

42 Results for the curvature model with Dc = 60º and α = 45º 70

A-1 Family of curves for the high conductivity channel model for λm1 = 115 m and different ranges of Tch and RL 82

A-2 Family of curves for the high conductivity channel model for λm2 = 162 m and different ranges of Tch and RL 82

A-3 Family of curves for the high conductivity channel model for λm3 = 256 m and different ranges of Tch and RL 83

A-4 Family of curves for the high conductivity channel model for λm4 = 303 m and different ranges of Tch and RL 83

A-5 Family of curves for the high conductivity channel model for λm5 = 397 m and different ranges of Tch and RL 84

A-6 Family of curves for the high conductivity channel model for λm6 = 444 m and different ranges of Tch and RL 84

A-7 Family of curves for the high conductivity channel model for λm7 = 513 m and different ranges of Tch and RL 85

CHAPTER 1

INTRODUCTION

Summary

Levees are structures created to prevent damage to infrastructure and civilization caused by floodwaters released by a river during times of high water flow. Due to the destructive nature of floodwaters, these structures are prone to several kinds of failure. One of the causes of failure is underseepage, where water flows through the soils underneath the levee and resurfaces on the landside. If the velocity of the water is high enough, it can erode the soil and start to create a problem called "backward erosion piping" where the erosion works its way back toward the river, creating a pipe that can eventually collapse. This can cause slope stability problems or drop the elevation of the levee crest, which can lead to overtopping and complete failure of the levee section.

Generally, backward erosion piping occurs in silty or sandy soils where erosion occurs easily with low water velocities. Therefore, levees with sandy foundations (or that have a partially sandy foundation) are more prone to this kind of failure. Alluvial river systems by definition contain lots of sandy and silty sediment, and therefore deposit lots of these sediments throughout their lengths. However, the nature of alluvial deposition creates variability in the levee foundations as a result of the several kinds of geomorphic features that are deposited. Sometimes it can be difficult for geotechnical site investigations to determine the presence or extent of said features, which can lead to the failure of the levee section.

Two of these features specifically tend to occur in levee alignments that are curved, instead of linear (as most levee alignments are treated during most current analyses). These two features are the point bar, essentially a sandbar that has been covered by subsequent fine grained deposition, and the meander scroll, which is a series of adjacent point bars separated by a clay "drape" that essentially isolates each point bar from water directly seeping into the next. The point bar and meander scroll are unique in that they exacerbate the effects of underseepage not only by placing sandy soil in the foundation but also by being within a curved levee section, which already concentrates the seepage.

The effects of point bars and meander scrolls on levee stability have not been numerically modeled. This research proposes to use a new reliability-based underseepage analysis method to model these effects. This new method, called the Response Surface-Monte Carlo method, was developed by John Rice and Lourdes Polanco (Rice and Polanco 2012, Polanco and Rice 2014). The method is implemented using a finite element analysis program to determine the effects certain geometric and hydraulic parameters of the point bar and meander scroll have on the seepage regime to develop a response surface, and then the probability density functions of these parameters will be used along with the response surface in the program @Risk to perform the Monte Carlo simulation.

Purpose

This study is part of a larger and broader research project designed to develop a method for determining the risk associated with levees over uncertain foundations. This

method will take into account subsurface geometry and geomorphic features that are not included in current analysis methods and are believed to increase the accuracy of the associated risk assessments. The study described in this document specifically considers the effects of point bars (a geomorphic feature associated with rivers) that intersect curved levee sections, especially their effects on the factor of safety with respect to heave and with respect to gradient at the landside toe of a levee.

Significance

As previously stated, this project is part of a much larger project that is meant to improve the analysis and design of levees. This specific research determines the effects of point bars and meander scrolls, two geomorphic features, on levee underseepage and establishes a way for a new method to analyze these features. This project provides two key elements to the larger project: 1) the development of a model for point bars and meander scroll deposits, and 2) the development of a method for incorporating the effects of levee curvature on the assessment of behavior of these deposits.

Organization

This thesis contains five chapters. The first chapter introduces the research and outlines the purpose and significance thereof. The second chapter is the Literature Review section, where studies of current and new methods for levee underseepage analysis are discussed, as well as the effects of levee curvature and the presence of certain geomorphic features within a levee alignment. The third chapter discusses the methodology used in analyzing geomorphic features to determine their effects on

underseepage, as well as how the knowledge obtained from this analysis is used to create a tool to determine the effects of any similar geomorphic feature on any given levee alignment. The fourth chapter discusses the particulars of the analysis and the creation of a “response surface” which is the tool mentioned previously. The fifth chapter is a conclusion of the results and analysis.

CHAPTER 2

LITERATURE REVIEWED

A literature review of publications pertinent to this study was performed to assess the current state of knowledge related to the subject. The literature reviewed is subdivided into four main topic areas and is presented below under these headings:

1. Current Levee Underseepage Analysis Methods
2. Response Surface-Monte Carlo Method
3. Effects of Levee Curvature
4. River/Point Bar Geomorphology

Current Levee Underseepage Analysis Methods

The most common method for analyzing most problems in geotechnical engineering is the deterministic analysis method. This method compares driving forces to resisting forces, and creates a ratio of the two, called the factor of safety (F). As it pertains to levee underseepage, the most common factors of safety that are calculated are the factor of safety against piping erosion and the factor of safety against heave. The factor of safety against piping is calculated by comparing the buoyant unit weight of the soil to the unit weight of water (this ratio is called the critical hydraulic gradient) and then dividing this ratio by the exit gradient of the water on the landside of the levee (Terzaghi 1922). The factor of safety against heave is calculated as the ratio of the total weight of

the soil overlying the point in question to the upward vertical hydraulic pressure of the water at that same point.

This deterministic type of approach is appealing because it computes a tangible value to compare with safe values to determine whether the levee will fail or not. However, the problem with this method is that it, in turn, requires that tangible values be input into an equation to calculate the factor of safety. Often these values have to be estimated with a large degree of uncertainty (Duncan 2000), as many parameters involved in these calculations cannot be determined by testing or field measurements.

One such deterministic method was developed by the U.S. Army Corps of Engineers (USACE) and is commonly called the "Blanket Theory." The blanket theory method consists of a series of closed-form equations that can be used to determine a factor of safety against heave within a simple geometry section. These equations require that the geometry being analyzed consist of a "blanket" layer of low permeability material underlain by a foundation layer of higher permeability material that stretches underneath the levee and into the river. Both of these layers are required to have uniform hydraulic conductivity through their respective layers, as well as a constant thickness (USACE 2005). This is one of the most commonly used methods for levee underseepage analysis.

Because of the uncertainty involved in determining values for certain parameters involved in levee underseepage analysis, probabilistic methods have been integrated into the design of levees by the USACE (USACE 2000). The most common of these probabilistic methods is the combination of the Blanket Theory equations with a First Order Second Moment Taylor series (FOSM method). This method uses a simplified

Taylor series that includes the most likely values and standard deviations of these values to determine the most likely value and standard deviation of the factor of safety against piping (Sleep and Duncan 2008).

Response Surface-Monte Carlo Method

Current analysis methods such as the Blanket Theory method are not able to account for the possibility of varying geometry within a levee foundation profile. To account for the possibility of variable geometry, Rice and Polanco (2012) and Polanco and Rice (2014) proposed the use of a Response Surface-Monte Carlo Method. This method is comprised of creating a response surface to describe the behavior of a model and then using a Monte Carlo simulation to generate the probabilities of certain behaviors occurring.

A response surface is comprised of parameters combined to describe the behavior of a given model (Xu and Low 2006, Low 2008). In the case of levee underseepage, these input parameters include hydraulic conductivities of respective soil layers, geometric parameters of the levee reach and features in question, and unit weights. The response surface is a relationship between the input parameters and seepage behavior developed from results from finite element analysis of levee reaches. The response surface is represented by a series of equations that can be used with a broader spectrum of geometries, hydraulic conductivities, and the other parameters that are considered.

To perform a Monte Carlo simulation from the results of the response surface, a Probability Density Function (PDF) must be created for each input parameter that describes the probabilities of the parameters over a range of possible values. Using both

the response surface and the PDFs, the Monte Carlo simulation can be performed to determine the likelihood of erosion initiation, described by the probability of achieving a certain factor of safety against heave of backward erosion piping (Rice and Polanco 2012).

This method was tested with several cases of levee profiles and compared to the FOSM Blanket Theory method by Polanco and Rice (2014). The results that could be compared demonstrated that the FOSM Blanket Theory is, to varying degrees, more conservative in its appraisal of the probability of unsatisfactory performance. However, two cases discussed in the paper could not even be accommodated by the FOSM-BT method, which further demonstrates the versatility of the RSMC method and its capability.

Effects of Levee Curvature

One other limitation of the current methods of analyzing levee underseepage is that they all assume that the analyzed levee section is linear. However, in most (if not all) river systems where levees are constructed, the river follows a series of meanders and has relatively few straight sections (Thorne, Hey, and Newson 1997). This fact is ignored in most analyses, and is often accounted for by simply increasing the factor of safety for the design calculations.

However, the effect of levee curvature on the erosion potential of a site is undeniable. Benjasupattananan (2013) demonstrated using finite element analysis that the effect of curvature can increase the head by as much as 1.5 times in the case of 180 degrees of curvature (see Fig. 1). The cause of this effect is the concentration of flow that

occurs due to the convergence of water flows on the outside of the curved levee section. The flow becomes radial instead of linear and this concentration of flow can be drastic in some cases, and can significantly increase the probability of failure of a levee section (Inci 2008).

To account for the effects of curvature, Meehan and Benjasupattananan (2012, 2013) proposed an axisymmetric Blanket Theory method that derived equations for an axisymmetric levee section similar to the way that the original Blanket Theory equations were derived. This approach provides a simple calculation tool for engineers (especially those already familiar with the USACE Blanket Theory equations) to use to predict the pressure head and factor of safety more accurately because of the inclusion of curvature. As demonstrated in Fig. 1, the axisymmetric case (the flat black line at approximate Normalized pressure head equaling 1.21) would give a conservative estimate of the factor

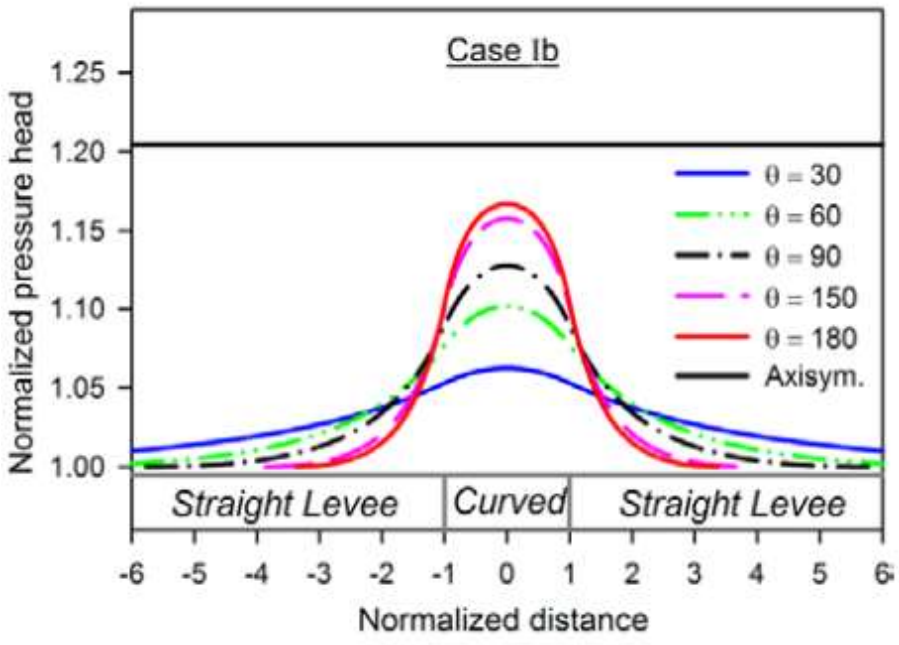

Fig. 1. Effect of levee curvature on pressure head

of safety, as it includes radial flow from all sides, not just from a partial arc over the degree of curvature as would exist in reality. Benjasupattananan demonstrated through the modeling of several levee alignments the effect of different degrees of curvature on the amount of flow that would concentrate on the landside of the levee. The modeling that Benjasupattananan performed on levee curvature greatly influenced the research subsequently discussed in this thesis.

The degree of curvature that had the closest result to the axisymmetric result was the 180 degrees of curvature, followed by a general trend of decreasing similarity as the degree of curvature decreases as a result of the decrease in flow concentration as the curved levee alignment becomes more similar to a rectilinear levee alignment. As the degree of curvature decreases from 360 (axisymmetric) to 0 degrees (rectilinear), the pressure head decreases correspondingly.

River/Point Bar Geomorphology

Levees are built as a flood control mechanism to ensure that populated areas do not get damaged by flood waters during high water events. Most of these populated areas of concern are concentrated around meandering river systems and therefore most of the levee systems are as well (Petroski 2006). For this reason, the focus of this research was on the effects of a particular aspect of alluvial geomorphology on the probability of erosion initiation near a levee.

This research was created based on the observations that have been made that geomorphic features can have a large effect on the piping erosion that occurs along levees that can eventually lead to failure or unsatisfactory performance of a levee reach or

system (Glynn and Kuszmaul 2010). The general composition of alluvial environments, as shown in Fig. 2, consists of a generally sandy foundation overlain by fine grained blanket deposits, with the possible inclusion of other geomorphic features. Several geomorphic features that are common in alluvial regimes include: point bars, meander

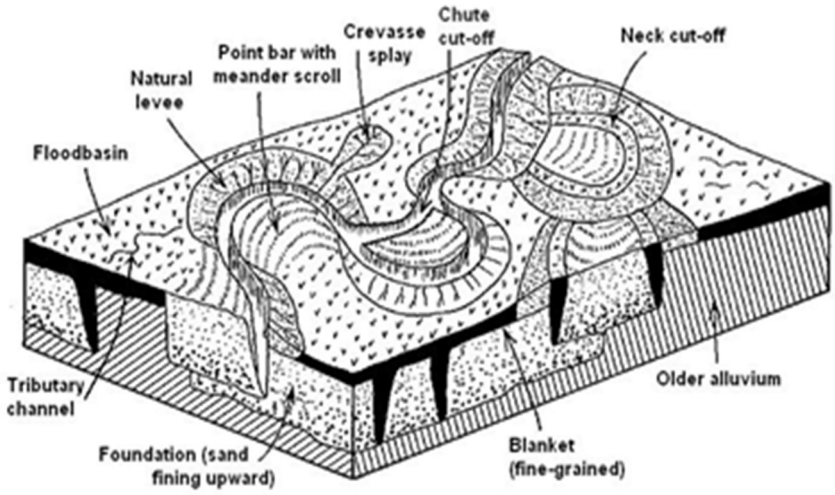

Fig. 2. Graphic of several geomorphic features, modified from Allen (1970)

scrolls, abandoned channels and crevasse splays (see Fig. 2). Each feature poses a unique problem for levee erosion and each contributes to changing the probability of piping erosion of the foundation of the levee reach where it is found.

A point bar is an alluvial deposit that occurs on the inside bank of a meandering channel, and normally consists of coarser material as it is deposited by rapidly flowing water. The coarser material is usually comprised of sand and gravel eroded from the opposite bank and carried from farther upstream (Nanson 1980). As the water collides into the outside bank of the river, it creates a helical circulation of the water that erodes

the outside bank, and then deposits that sediment on the inside bank as it reaches a section of flow that offers higher resistance (the separation zone) and causes the water to slow down and release its suspended sediment. This process is depicted in Fig. 3. As the channel migrates laterally, the process tends to deposit finer sediment (mostly silt) on top of the existing bar, and eventually overbank deposits create the blanket layer that levees are often constructed on top of (Nanson 1980). Because of this deposition of finer

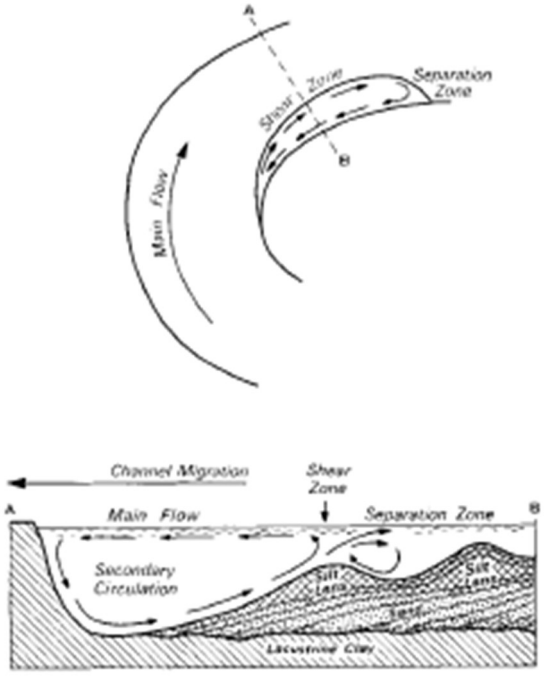

Fig. 3. Cross-sectional depiction of water flow and point bar initiation in alluvial rivers, from Nanson (1980)

sediments, often the existence of a point bar can go unnoticed during levee construction which can lead to the problems of piping erosion that were previously mentioned. The main components of the point bar that contribute to higher risk of failure are the coarse

sediment that can lead to a concentration of flow within the point bar, as well as the effect of thinning the blanket layer which can lead to a higher chance of heaving of the blanket.

Meander scroll bars are another geomorphic feature, very similar and related to the point bar feature previously mentioned. The meander scroll is essentially a series of point bars separated by a layer of finer sediment, in a "ridge and swale" pattern as shown in Fig. 4 (Woolfe and Purdon 1996). How these features are formed has been debated and several hypotheses have formed. They all start, however, with a point bar formation as described above. After the initial point bar is formed, one hypothesis is that flow zones

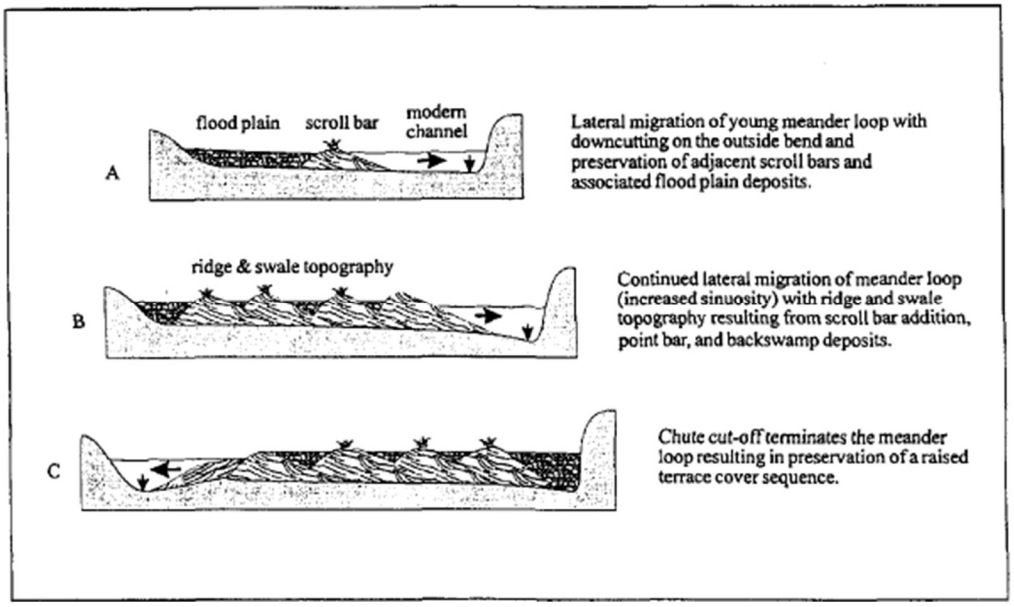

Fig. 4. "Ridge and swale" topography characteristic of meander scrolls, from Woolfe and Purdon (1996)

form naturally above a point bar, which leads to different ridges of sediment getting deposited. These deposits then influence the location of these zones, which leads to more ridges forming and the formation of the scroll bar progresses in this manner (Nanson 1980).

The second theory is that in rivers where scroll bars form, there are two size ranges of bedload that would cause two separate ridges to start forming within a certain part of the river (Nanson 1980). The third theory is that certain meander scrolls can initiate as a result of trees or other objects getting trapped on a point bar. These obstructions cause the flow to slow down and cause the water to release its sediment, which results in deposition around the obstruction until the obstruction is covered, and then a new ridge is formed (Nanson 1981). These features cause the same problems as the point bar - they thin the blanket which leads to an increased probability of failure by heave, and they can also create a concentration of flow that leads to higher pressure being applied to the blanket layer, as well as an increased potential for piping erosion. Fig. 5

Fig. 5. Photograph of the topography above a meander scroll, from Woolfe and Purdon (1996)

shows a photograph of the "ridge and swale" topography created by these features (Woolfe and Purdon 1996).

Fig. 6 depicts the layers of fine sediment (also called clay drapes) that sometimes form in between successive point bars to create the meander scroll. It also describes the formation of these geomorphic features in considerable detail, including the accumulation of overbank deposits that eventually cover up these features with blanket sediment (Gagliano and Van Beek 1970, published in Saucier 1994).

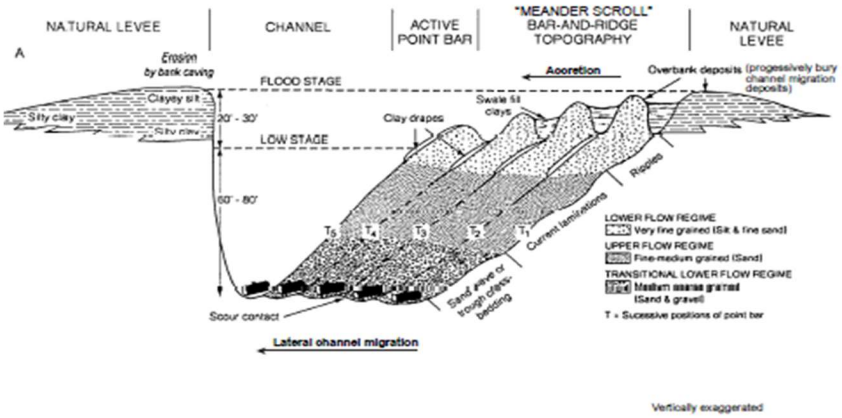

Fig. 6. Depiction of clay "drapes" that accumulate in between subsequent point bars to create a meander scroll, from Gagliano and Van Beek (1970, published in Saucier 1994)

CHAPTER 3

METHODOLOGY

Problem Statement

Currently, the most common probabilistic method for determining the resistance of a levee to failure by underseepage is the use of the U.S. Army Corps of Engineers Blanket Theory equations along with a first-order, second-moment analysis. The Blanket Theory equations are used to calculate a factor of safety against heave, based on a simple soil profile of a foundation layer overlain by a blanket layer. Each of these layers is assumed to have a uniform thickness, as well as an uninterrupted length stretching toward the landside of the levee. A few modifications allow for modeling layers pinching out. In conjunction with this Blanket Theory method, the First-Order Second-Moment Taylor series has been applied to create a probabilistic method. The main problem with this approach is that the equations can only apply to soil profiles with this very simple geometry, and any other profile is therefore excluded from being able to be analyzed with this Blanket Theory method.

Naturally occurring fluvial geomorphic features have been observed to have an effect on the performance of levee sections as they change the subsurface geometry and foundation continuity (Glynn and Kuszmaul 2010). Features like point bars, meander scrolls, and abandoned channels can affect flow concentrations and locally change the thickness of blanket layers or the permeability of the foundation layer and thereby cause a change in hydraulic gradients and pressures. Abandoned channels are formed by either tributary cross streams that have changed course or by a change in course of the main

channel. Point bars and meander scrolls are usually coarse-grained sand and gravel deposits that form on inside bank of curved river sections. The propensity of point bars and meander scrolls to form on curved levee sections adds additional complexity in analysis, as levee curvature can also affect the hydraulic gradients and pressures.

A new method called the Response Surface-Monte Carlo (RSMC) method makes it possible to incorporate the variability of subsurface geometry as well as soil property parameters that influence the seepage and pressures that build up on the landside of the levee. The RSMC method works by combining parameters to simplify and describe the behavior of a model, and then running a Monte Carlo simulation using probability density functions representing the combined parameters (Polanco and Rice 2014). This simulation can be performed to determine the likelihood of erosion initiation, described by the probability of achieving a certain factor of safety (Rice and Polanco 2012). This method can be used to calculate the probability of erosion initiation within a certain levee reach by either piping or heave and allow comparison between different reaches with different geometries and other parameters. This method not only accounts for non-uniform geometry but can also account for failure modes other than just the piping erosion initiation that is included in the FOSM-BT method. The main failure mechanism observed in many levee reaches is that of heave, where water pressures build up underneath the relatively impervious blanket layer, causing the layer to heave upward and crack, which then allows the piping erosion to initiate and the sediment to flow out through the crack onto the surface (Wolff 2002).

The focus of this study will be to analyze the effects of subsurface geometry and other parameters on the behavior of a levee reach or system. The geometry and

characteristics that will be studied will be those of naturally occurring point bars and meander scrolls, as these geomorphic features are very similar and cause similar effects on the performance of levee sections. To analyze these features, the three dimensional finite element analysis (FEA) seepage program SVFlux (SoilVision, 2014) was used. The analysis from SVFlux will be used to develop a response surface that will relate the important parameters that affect the behavior of the point bar or meander scroll. Probability Density Functions (PDFs) will then be developed for the important parameters. The response surface and pdfs will then be used in a Monte Carlo simulation to determine the likelihood of unsatisfactory performance (Polanco and Rice 2014).

Overview of Methodology

To be able to use the RSMC method, the behavior of point bar and meander scroll underseepage had to be studied and understood so that a response surface could be developed. Parametric analyses were performed to understand the behavior caused by the point bar and meander scroll on the levee underseepage by isolating and varying different parameters significant to the study. From the parametric analysis, important parameters were chosen and combined to reduce the number of parameters in the response surface and make the number of analyses feasible. Curvature of the levee section was also studied to determine its effects, since most point bars and meander scrolls are deposited along curved river sections.

To start the process of creating a response surface, a general point bar model was created. After collecting data on the characteristic soil properties and geometry of naturally occurring point bars along the Sacramento River, average values from this data

were used to create the general model. This initial model was created to serve as a starting point for parametric analyses, and was intended to be representative of real conditions found in levee foundations.

After the collection of the data and creation of the general model, parametric analyses were performed on the model by changing parameters to determine what parameters were to be used for the response surface. The development of the response surface was done by combining the parameters that were found to have significant effect on the hydraulic head within the point bar. The response surface was also verified for its effectiveness by back calculating heads with a finite element analysis program using the parameters that were used to create the response surface.

The effects of levee curvature were originally considered for inclusion of the response surface as well. The radius of curvature was the first parameter studied, to determine if different radii of levee alignments have different hydraulic head regimes. The amount or degree of curvature was also studied to determine its effect on the hydraulic head in the point bar or meander scroll. It was later determined that the effects of curvature could be applied to the model as a correction factor after the response surface analysis.

Response Surface Methodology

The methodology developed by Rice and Polanco (2012) was used to develop a response surface and run the Response Surface-Monte Carlo simulation with the point bar and meander scroll geomorphic features. The steps that were followed are listed below:

Step 1 - Finite Element Model Setup. This step will be described in detail in the following chapter, but essentially a base model needs to be created that can be modified for parametric analysis to be able to develop a response surface. The geometric dimensions of this model were determined through research of levee alignments and geomorphic features in the Sacramento River region of California. Soil properties were estimated based on deposition processes of the soils involved as well as geotechnical soil property estimates. Boundary conditions were selected based on likely flood event properties in the Sacramento region. After collecting these parameters, the model was constructed in the three-dimensional finite element analysis program SVFlux (SoilVision, 2014).

Step 2 - Parametric Analysis. Using the model created in step one, individual parameters were isolated and varied to determine their effects on the resulting hydraulic head and exit gradient values found on the landside toe of the levee, where seepage would be of concern. This analysis allowed an assessment of the relative importance of all input parameters to the model. From this analysis, the parameters that significantly affect the model outcome were identified. Also, parameters that have negligible effect on the outcome were identified. This will be discussed in further detail in the following chapter.

Step 3 – Combination of Parameters. The results of the parametric analyses are used to reduce the number of parameters for the response surface. This is done by eliminating parameters that are found to be insignificant to the results, and combining the remaining parameters into three combined parameters that adequately define the behavior of the simplified model.

Step 4 - Response Surface Generation. Using the simplified model, a response surface is created for the three combined parameters. This was done by generating several graphs, each with several curves that relate the parameters chosen to the heads or gradients that were calculated with SVFlux (SoilVision, 2014), called a family of curves. Each graph held one of the combined parameters constant while changing the other two to relate their effect on the resulting hydraulic head or exit gradient. This variation occurred for the full range of physically possible values for each parameter. For example, the hydraulic conductivity of the blanket was varied within its natural range of hydraulic conductivities, and the hydraulic conductivity of the foundation will also be varied within its natural range and so on.

Step 5 – Levee Curvature. To account for the curvature of the levee sections that point bars affect, a hydraulic head multiplier was developed for varying degrees of curvature. Derived from Benjasupattananan 2013, curves were established based on several degrees of levee curvature, ranging from 0 to 180 degrees. These curves were normalized so that hydraulic head for a straight levee section could be simply multiplied by a factor taken from the curves to determine the head that would be calculated in a curved levee section.

Step 6 - Verification of Combined Parameters. The combined parameters chosen in step three were verified for how accurately they approximated the full model. This was achieved by calculating hydraulic head using the simplified model parameters, and then using the same parameters as inputs for the FEM program to calculate the hydraulic head with the program. The results of both calculations were then compared to ensure that the results of both methods were similar.

Step 7 - Curve Fitting. Once the curves were generated for the general cases, polynomial curve fitting was applied to each curve to develop equations representing the response surface. Values between the curves were to be calculated by interpolation between the curves in the Monte Carlo simulation.

Step 8 - Develop Probability Density Functions. To be able to apply the combined parameters to the Monte Carlo simulation, Probability Density Functions (PDFs) were created for each of the significant parameters. This allows for the random sampling of the Monte Carlo simulation to occur.

Step 9 Spreadsheet and Programming Modification. To be able to set up the Monte Carlo simulation part of this project, a spreadsheet was created to include the response surface equations and interpolation program, probability density functions, and output tables for the analysis. The interpolation program was used to calculate hydraulic head or exit gradient values from any arrangement of input values. It interpolates between the equations from the response surface to allow the user to input parameters from any levee reach in question and still run the Monte Carlo simulation.

Step 10 - Monte Carlo Simulation. After assembling the PDFs and interpolation program into a Microsoft Excel spreadsheet, the program @Risk by Palisade is used to perform the Monte Carlo simulation. The simulation is generally performed once, running 10,000 iterations to produce a result of probability of unsatisfactory performance based on the input parameters.

CHAPTER 4

ANALYSIS OF DATA

This chapter describes how the previously described methodology was applied to the problems of levee curvature, point bars, and meander scrolls in the foundation of a levee alignment.

Data Collected

Every river system varies in its depositional environment due to changes in hydraulic and geologic properties such as channel size, flow volume and velocity, sediment source, and a multitude or other factors. These factors affect the size, shape, and composition of the geomorphic features that are deposited within this geologic environment. To be able to analyze point bars and meander scrolls, a generalized model had to be developed that has the capability of incorporating the wide range of values that are possible for all of the input parameters controlling the model outcome. However, by building a model that mimics the general underseepage behavior of the geomorphic feature, the model can then be simplified for use in the Response Surface-Monte Carlo analyses while still incorporating the effects of all parameters. This simplified model can then be used to construct a response surface that describes the variation of the geomorphic feature's behavior with changing input parameters. Data was collected from actual surficial geologic mapping to find a range of parameters within which to develop a general finite element model and eventually a response surface. It is important to note that the creation of a general model was simply a tool to understand the behavior and

create the response surface. The parameter values that were chosen were all alternately changed in parametric analyses to determine their respective importance.

An area that was determined to be a representative example of levee/river interaction was in the “pocket” area of south Sacramento. William Lettis and Associates (2008) developed a surficial geologic map of this area that includes many of the geomorphic features mentioned earlier in this work, including crevasse splays, abandoned channels, meander scrolls and point bars. These features were measured to determine a representative radius of curved levee section to use for point bar analysis, as well as meander scroll analysis. From the Lettis and Associates map, three Holocene meander scroll features and one point bar feature were identified. According to Lettis and Associates (2008), these features were formed during the current geologic epoch, but before recorded history. The most important property that could be extracted from this

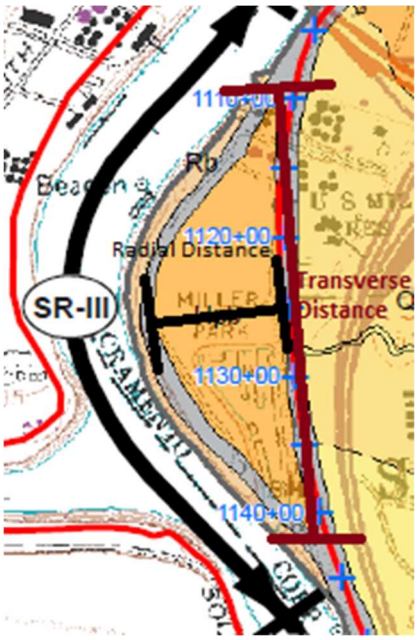

Fig. 7. Convention for radial distance, modified from William Lettis and Associates (2008).

map was the radial distance (shown in Fig. 7) from the front to the back of the point bar, which determined the radius of our characteristic curved levee alignment. The width of the point bar transverse to the radial width was also measured for classification of these features. The aforementioned features can be found on the following map (Fig. 8) and each has the respective following properties:

- Point bar 1 - Surveyed between stations 1105+00 and 1145+00, with a radial width of 0.2 miles and a transverse width of 0.62 miles.
- Meander Scroll 1 - Surveyed between stations 1270+00 and 1320+00, with a radial width of 0.25 miles and a transverse width of 0.73 miles.
- Meander Scroll 2 - Surveyed between stations 1380+00 and 1450+00, with a radial width of 0.28 miles and a transverse width of 1.04 miles.
- Meander Scroll 3 - Surveyed between stations 1540+00 and 1610+00, with a radial width of 0.25 miles and a transverse width of 1.23 miles.

The average of the radial width of these four features is 0.245 miles, or 1293.6 feet. For simplification, this was rounded up to 1300 feet. for the radius of the main point bar. Although this radius was chosen for the general model, parametric analyses were performed to determine the effect that changing the radius had on the behavior of underseepage beneath the levee in this curved section. This radius was simply chosen for the general model that could be used while changing other parameters that affect the levee underseepage behavior during the development of the response surface.

These parameter values were extracted from the geomorphic data about point bars and meander scrolls so that an initial, general model could be created in a finite element

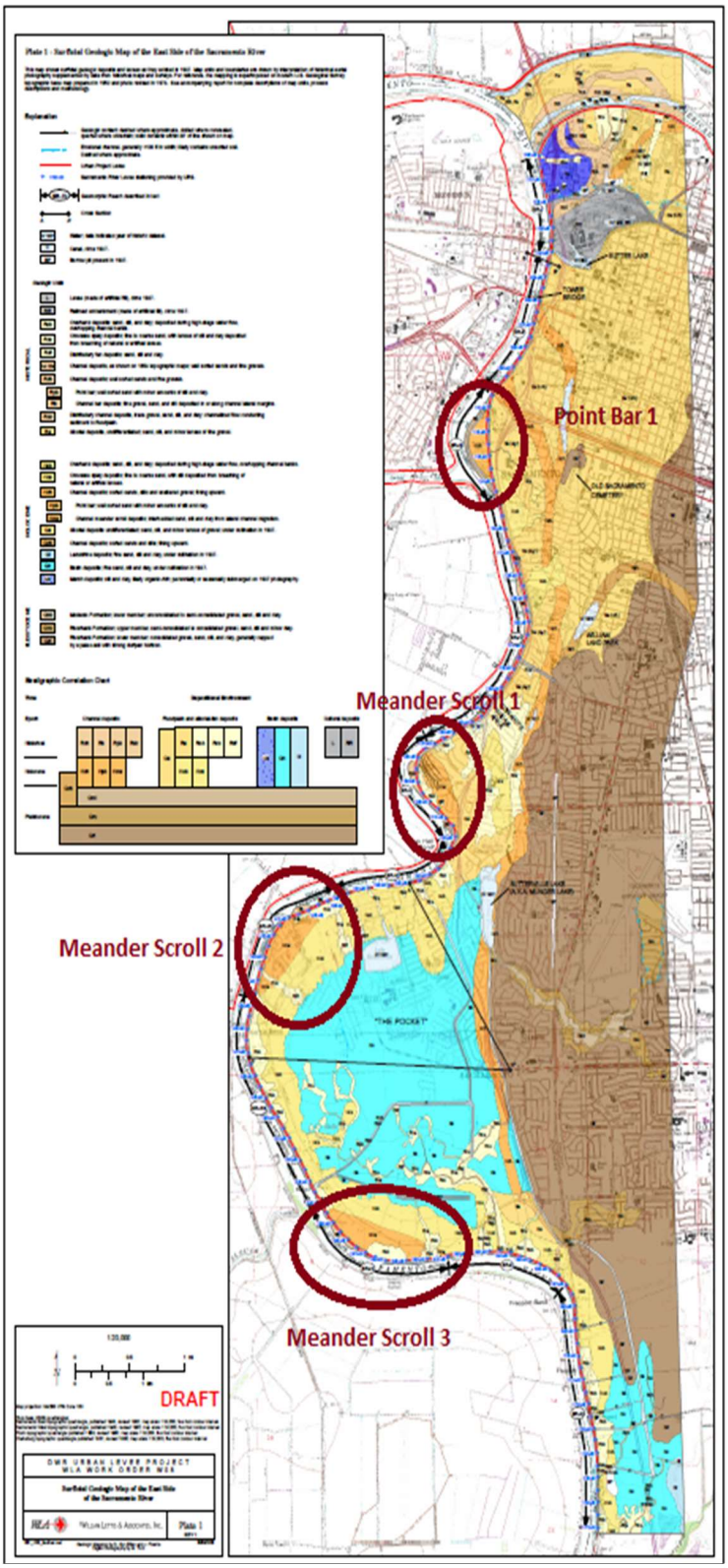

Fig. 8. Map created by William Lettis and Associates (2008) outlining the locations of point bars and meander scrolls in the Sacramento area

program to be a starting point for parametric analysis. After determining the radius of levee curvature to be used, a thickness needed to also be determined for the point bar. Using the geologic mapping results of Lettis and Associates (2008), it was determined that an acceptable point bar or meander scroll thickness would be 10 feet, with 25 feet of blanket overlying this deposit (see Fig. 9). The width of the point bar for the general model was determined to be 100 feet, and the cross section of the bar was modeled as rectangular. Obviously this is a simplification of the geometry, but one that was decided would not significantly affect the processes or behaviors being studied as long as the thickness of the blanket and the height of the point bar were representative of reality.

Hydraulic conductivities also had to be assumed for the materials, and this was done by using the Soil Conservation Service (USDA SCS 1993) estimations and converting them into feet per second to meet the input requirements of SVFlux (SoilVision, 2014). For the point bars, which are usually granular due to their depositional process, a hydraulic conductivity of 10^{-5} feet per second was chosen. For the semipervious blanket, 10^{-7} feet per second was chosen, and for the levee 10^{-10} feet per second was chosen to model the levee as essentially impervious. The blanket layer predominantly undergoes seepage in the vertical direction and the foundation undergoes horizontal seepage, thus anisotropy in both layers was considered to have no significant effect on underseepage and the main model was chosen to have no anisotropy in any direction. Another factor that affected this decision was the fact that since the hydraulic conductivity controlling the behavior is in the direction of the flow, the flow in any of the materials that affects the analysis is generally unidirectional.

The boundary conditions that were chosen to be used with the model were designed to model flood conditions that have a one percent chance of occurring in a given year (the 100-year flood) on the Sacramento River. For this reason, a head of 22 feet was chosen to be applied on the riverside of all levee sections, while maintaining a head of 0 feet on the landside at the ground surface. The levee section was represented with a "zero flux" boundary over the top of the levee footprint since all of the flow relevant to this

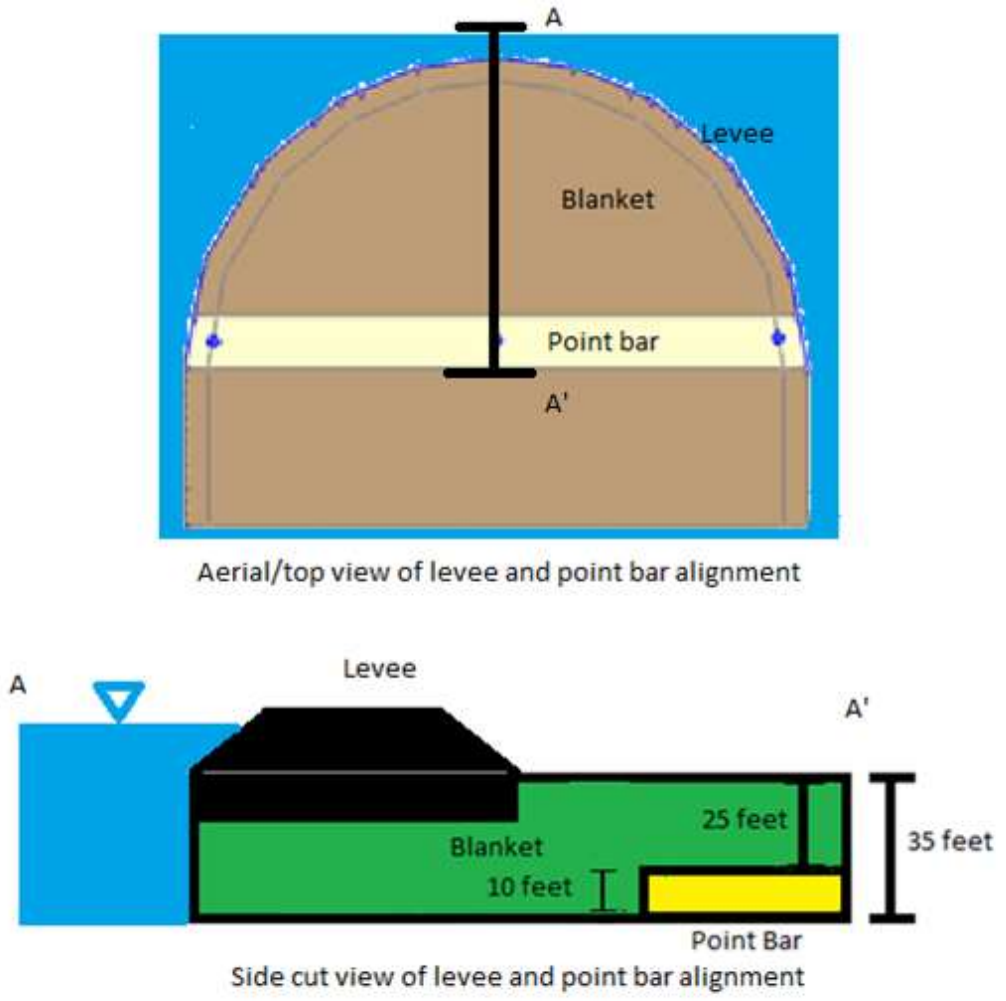

Fig. 9. Top and side views of the geometry of the point bar and levee alignment, not to scale

study was underseepage. The landside ground surface was modeled with a zero pressure boundary condition.

Parametric Analysis

The parametric analysis was initiated with the use of the two-dimensional finite element analysis program SLIDE created by RocScience. Several analyses were performed as a simplified study on the effects of point bars within the levee foundation. Sections were analyzed with the point bar running both longitudinally and transversely to the levee alignment direction (see Fig. 10 and 11). The main purpose of these analyses was to obtain a simplified understanding of how the point bar deposit affects the seepage regime in the two configurations in order to assist in understanding the three-dimensional flow regime.

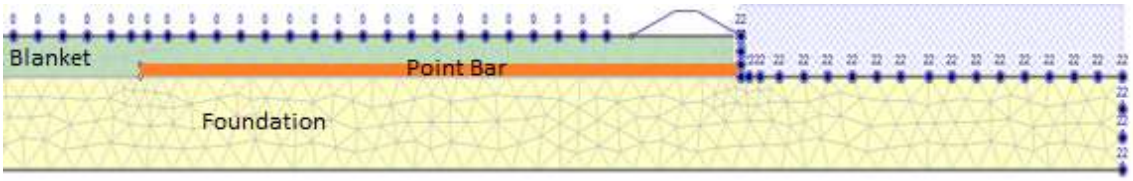

Fig. 10. Two-dimensional model of the longitudinal representation of the point bar

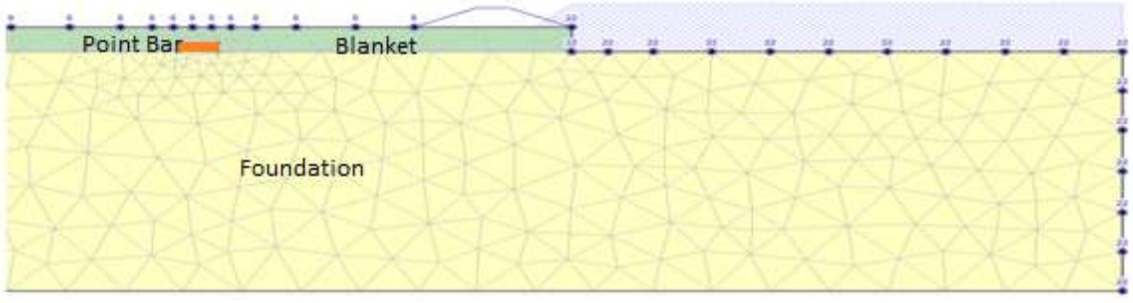

Fig. 11. Two-dimensional model of the transverse representation of the point bar

The two-dimensional analyses were done to better understand the two main flow regimes isolated one from another (there is radial flow that occurs from all sides of the levee alignment, and then specific concentrated flow through the point bar from the sides). The parameters that were varied during this analysis were the location of the point bar with respect to the levee, the thickness of the point bar, the thickness of the overlying blanket, the thickness of the foundation material underlying the point bar, the slope of the landside blanket, the hydraulic conductivity of the blanket, the hydraulic conductivity of the foundation and point bar which were considered to be the same due to the depositional processes that form point bars and foundation layers, as well as the ratio of the two hydraulic conductivities (blanket and foundation or point bar).

The location of the point bar affects the hydraulic head, but the effect was exactly as expected - as the location of the point bar moved farther away from the levee in the landside direction, the hydraulic head in the point bar decreased. This is a result of head loss in the foundation material as well as leakage of the head through the semipervious blanket layer above the foundation. So the critical case in our analysis is where the location of the point bar coincides with the levee toe, where the head would be the highest.

The thickness of the point bar was also studied to determine its effect on the hydraulic head. Maintaining a constant blanket thickness while increasing the thickness of the point bar has a negligible effect on the hydraulic head, and therefore it was concluded that point bar thickness is not an important parameter to consider when calculating hydraulic head in two dimensions. However, if maintaining total thickness of

landside materials constant, changing point bar thickness would require a corresponding change in blanket thickness, and the effects of changing blanket thickness are discussed below.

The thickness of the blanket has an interesting effect on the head calculated within the point bar. As the thickness of the point bar is held constant and the thickness of the blanket decreased, the head actually decreased slightly due to leakage, which is gradual seepage through the blanket layer as water travels through the foundation. The overall effect is not enough to counteract the decrease in the factor of safety with respect to heave caused by the thinning of the blanket.

The foundation thickness, unless it is decreased to a thickness that would amplify end effects, has no effect on the hydraulic head within the point bar. The foundation material and volume are such that the flow capacity of the foundation will always be much greater than the capacity of the blanket layer, and therefore is only considered to make sure that its thickness is sufficient to eliminate end effects from skewing data.

The slope of the landside blanket away from the levee was analyzed because in certain cases there are locations where a point bar is located underneath a landside depression where the blanket gradually slopes down on the landside. The analysis of this case seems to have similar effects on hydraulic head as the blanket thickness, because essentially what is occurring is a gradual thinning of the blanket across the entire landside of the levee to an arbitrary point where the thinning stops. If the point bar is located near the point where the blanket is thinnest, the factor of safety with respect to heave becomes significantly lower because the blanket is so thin at that point, but the head has usually decreased substantially due to head loss and leakage (since the blanket is normally

thinnest at the point farthest away from the levee). These results demonstrate that the slope of the landside blanket away from the levee does have an effect on hydraulic head and has the greatest effect on levee performance when paired with the location of a point bar.

Individual hydraulic conductivities of the materials that make up the foundation, blanket, and levee all have expected effects on the hydraulic head regime - as the hydraulic conductivity of the levee is increased, more seepage occurs through it instead of underneath it, and therefore the head in the point bar decreases. As the hydraulic conductivity of the blanket increases, more leakage occurs through it and also decreases the head in the point bar. As the hydraulic conductivity of the foundation increases, less leakage occurs through the blanket, and therefore head increases in the point bar. However, the real factor that determined the amount of head in the point bar was the hydraulic conductivity ratio of the foundation to the blanket. It is assumed that the levee hydraulic conductivity is going to be significantly lower than the blanket and the foundation (since the point of this study is to determine the effects of underseepage in a levee alignment), and therefore its hydraulic conductivity is not considered when looking at the ratio. The assumed initial ratio was two orders of magnitude, or 100. As the ratio is increased from 100, the hydraulic head in the point bar increases as well as a result of the lowered leakage as either the blanket hydraulic conductivity decreases or the foundation hydraulic conductivity increases. As the ratio decreases, the head also decreases as leakage increases.

The parametric analyses were also performed in the three-dimensional model, created in the program SVFlux (SoilVision, 2014). Several other parameters were also

analyzed, including the radius of curvature of the curved levee section, the degree of curvature, the length of the point bar, the width of the point bar, and hydraulic conductivity anisotropy of the point bar material. The results of these analyses are presented in the following paragraphs.

The first parameter analyzed using the three-dimensional finite element analysis program was the length of the point bar within the land section of the curved levee section. This was achieved by initially creating the 180-degree model, and putting a point

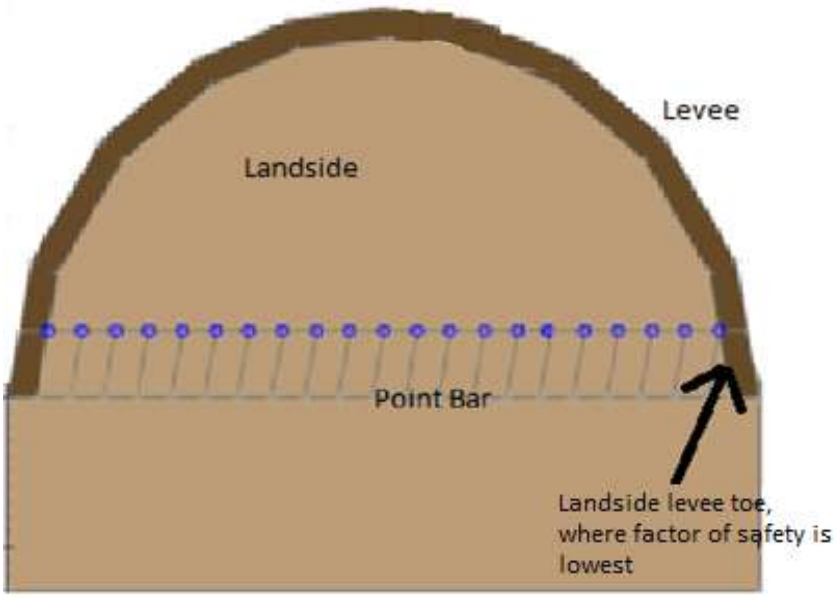

Fig. 12. A representation from SVFlux of how the point bar was shortened in this section of the experiment

bar across the span of the curved levee section. Then, the point bar was divided into discrete sections and progressively shortened by one unit in each run of the model (see Fig. 12). During each run, the head was calculated in several places along the point

bar, just below the blanket layer at the top of the point bar. The point where the head was calculated that was of the most interest was the entry point where the point bar crosses underneath the levee on the landside where the factor of safety is the lowest due to the hydraulic head being the highest at this point on the landside. This was calculated for all lengths of the point bar, and it was found that the head within the point bar changed very little as a result of shortening the point bar (see Fig. 13).

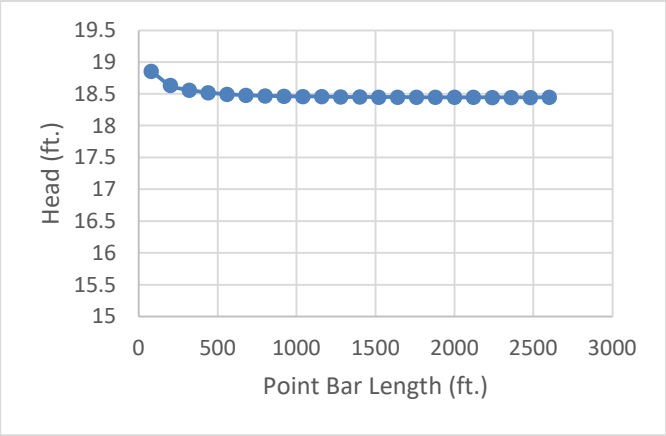

Fig. 13. Plot showing the effect of the point bar length on hydraulic head at landside levee toe

The second parameter analyzed was the angle of incidence of the point bar into the curved levee section (see Fig. 14). Initially, the model was set up to have an angle of incidence of 90 degrees. The model was altered to account for several different angles ranging from 20 degrees to 90 degrees. This effect of the angle of incidence on the head calculated in the point bar is demonstrated in Fig. 15.

The hydraulic conductivity (permeability) ratio was again studied (see Fig. 16) in the three-dimensional analysis and was found to have a significant impact on the hydraulic head and gradient through the blanket. As the hydraulic conductivity ratio

increased, the hydraulic gradient also increased as a result of the decrease of leakage into the blanket as the water traveled toward the point bar. As the hydraulic conductivity of the blanket decreased, the water almost exclusively traveled through the foundation and

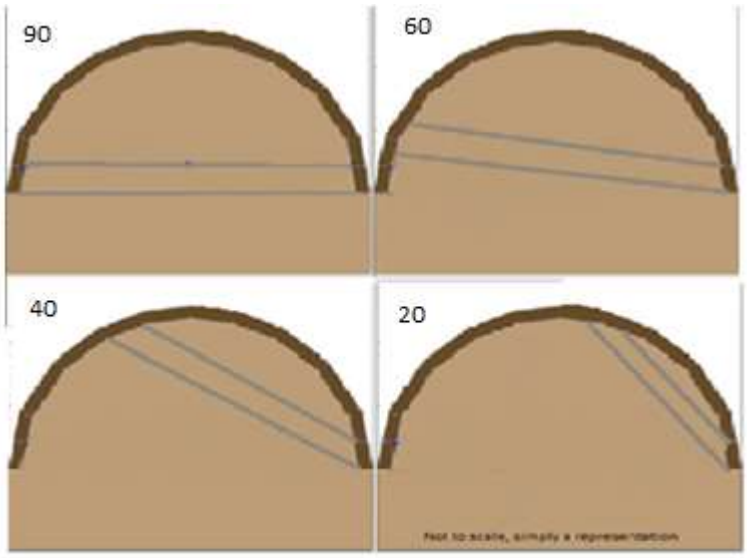

Fig. 14. From SVFlux, showing the convention for measuring the angle (in degrees) of entry of the point bar. The shape in between the gray lines represents the point bar

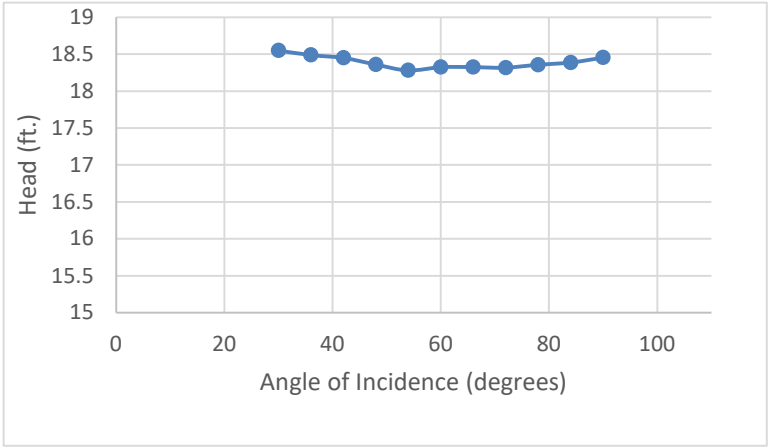

Fig. 15. Angle of incidence vs. hydraulic head at landside levee toe

into the point bar, losing very little head until it reached the point bar, which increased the hydraulic gradient.

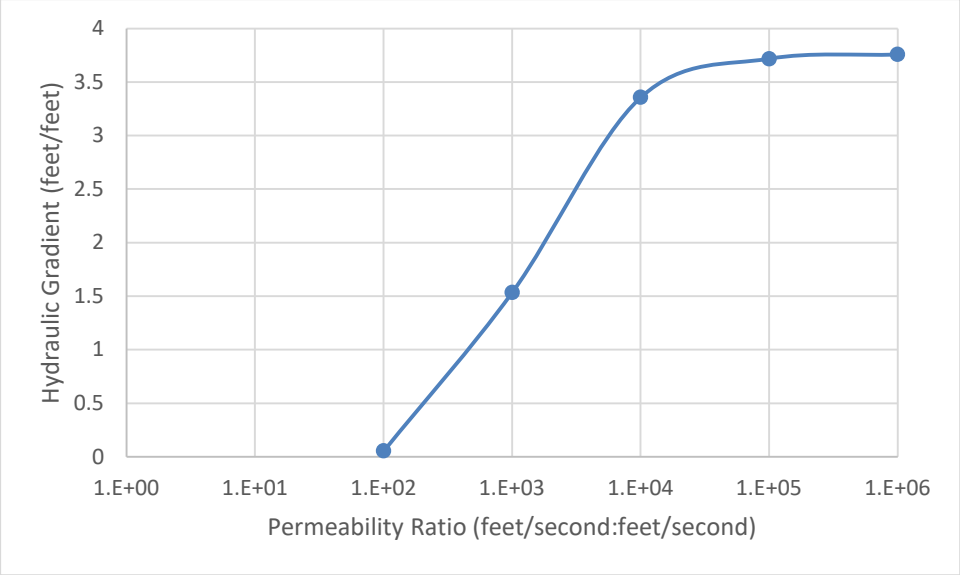

Fig. 16. Hydraulic gradient vs. permeability ratio of point bar to blanket, with a blanket permeability of 1 x 10^{-7} feet/second

Radius and degree of curvature of the curved levee section were also studied with the existence of a point bar underneath the section (see Fig. 17). Degree of curvature is simply the amount, in degrees, that the levee section curves along its alignment. A levee section with 180 degrees of curvature is a semicircle, and a levee alignment with 0 degrees of curvature would be a simple, straight levee section. To test the effects of curvature on the hydraulic head within the point bar, several degrees of curvature were analyzed while keeping the radius of curvature constant. When using a hydraulic conductivity ratio (of point bar to blanket) of 100 or less, the effects of levee curvature were negligible. However, using a ratio of 1000 showed that hydraulic head steadily

increased underneath the toe of the levee as curvature increased. Increasing curvature increases the amount of flow that can concentrate in a certain spot as the flow comes from several directions at once instead of just one direction, as in the case of a linear levee alignment or two-dimensional analysis. The lower degrees of curvature (like 30 degrees) most closely emulate a linear levee alignment and therefore the head difference

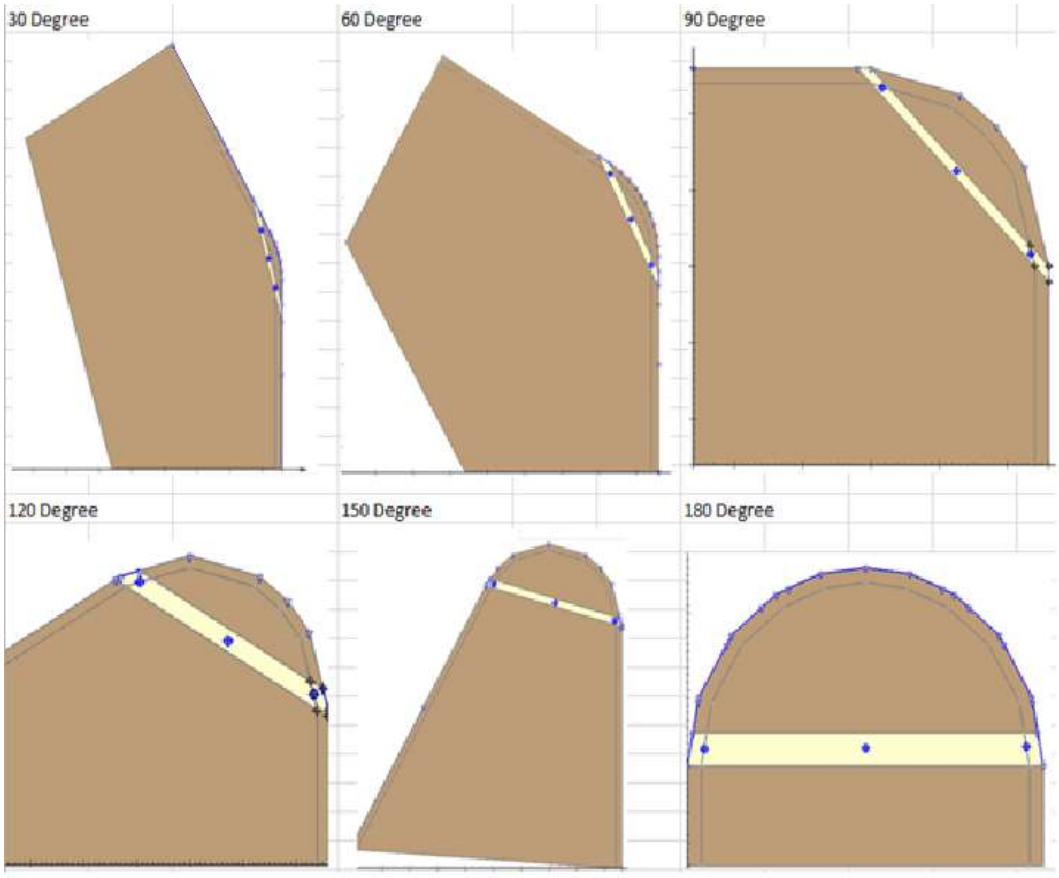

Fig. 17. Representations from SVFlux of the degrees of curvature. The yellow region represents the point bar

is small. However, larger degrees of curvature (like 180 degrees) have a larger head difference when compared to the linear levee alignment hydraulic head.

The radius of curvature of the levee alignment was also studied to determine its effects on the hydraulic head regime in the foundation and point bar (see Fig. 18). The effect in the middle of the point bar was very pronounced, with the hydraulic head ranging from 0.01 feet to 18.2 feet in the range of values that were studied. The general

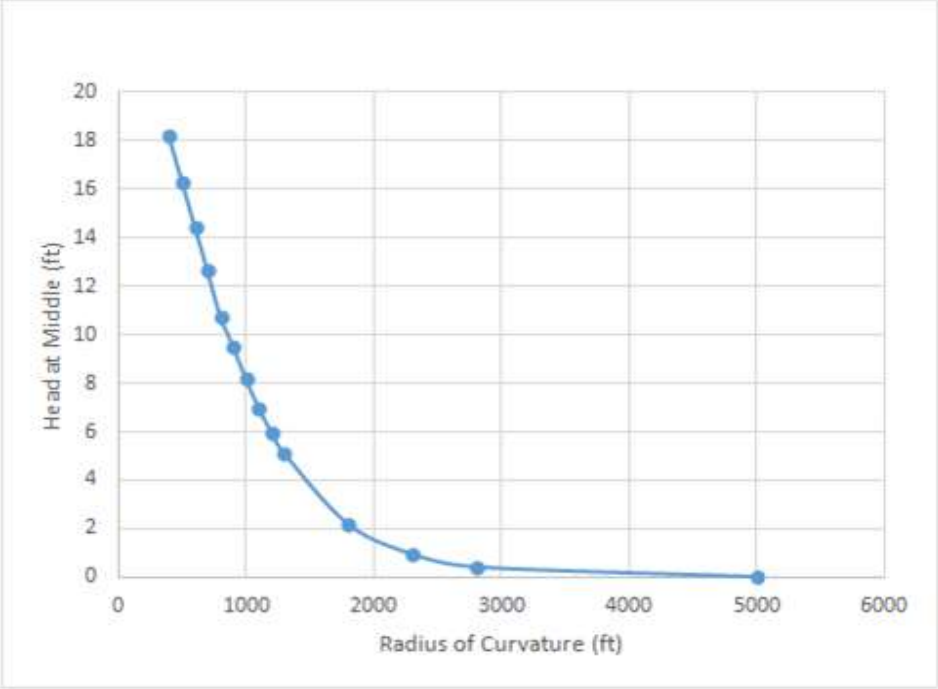

Fig. 18. A chart showing the effect of the radius vs. the head calculated in the middle of the point bar

trend of the relationship is an inverse function, with the head decreasing toward an asymptote representing zero change from the linear levee as radius of curvature increased, and likewise increasing toward an upper bound as the radius decreased toward

zero (in this case the upper bound would be 22 feet the boundary condition on the riverside of the levee).

The head underneath the levee toe was also calculated using the finite element program, and the shape of the trendline was similar although the head differential was less dramatic (see Fig. 19). The increase of head as the radius decreased was caused by the concentration of flow caused by the radial nature of the levee alignment. Likewise, the point where the curvature ceased to have an effect on head was caused by the radius being sufficiently large to effectively produce the same results as a linear levee alignment.

Another parameter that was analyzed to determine its effect on the head regime within the levee alignment was the existence of multiple adjacent point bars. As

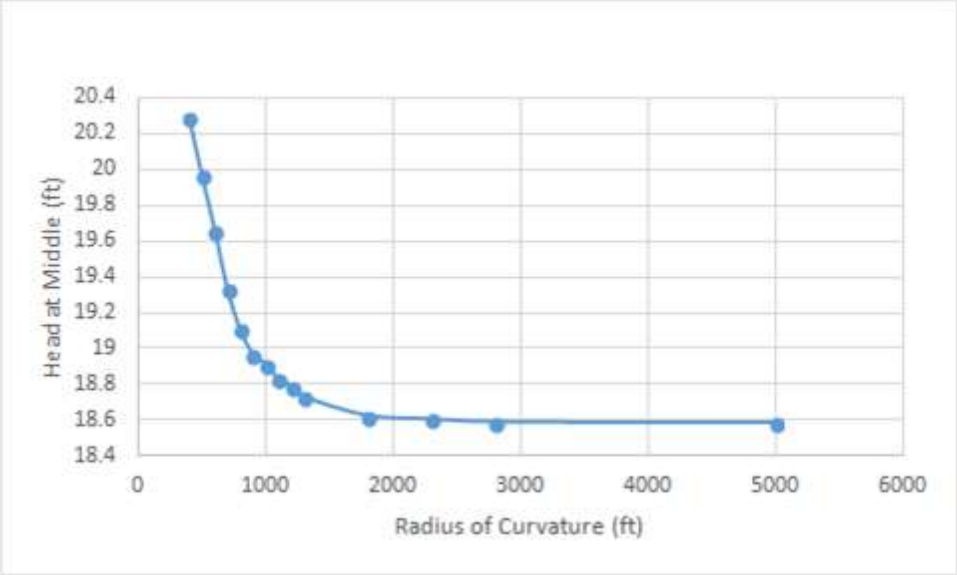

Fig. 19. A graph showing the effect of the radius on the head calculated in the point bar directly below the landside levee toe

discussed in Chapter 2, the nature of certain depositional environments can lead to the creation of meander scrolls, which are a series of point bars separated by a thin "drape" or layer of clay between each subsequent point bar. These clay drapes are low permeability seepage blocks that essentially isolate each point bar from the other. A parametric analysis was performed using a series of models to assess the effects of several geometric parameters with multiple point bars. The base model had a radius of 1300 feet and 180 degrees of curvature. To establish one extreme case of the meander scroll geometry, the first clay drape width was chosen to be 80 feet, meaning when there were three point bars underneath the levee alignment, they were spaced 80 feet apart. The results are shown in Fig. 20. The head difference is less than a tenth of a foot between the alignment with one point bar and the alignment with three point bars, so in this case the difference was negligible.

This same process was repeated for a levee alignment with the same, 1300-foot radius but only 90 degrees of curvature. The results, shown in Fig. 21, were very similar

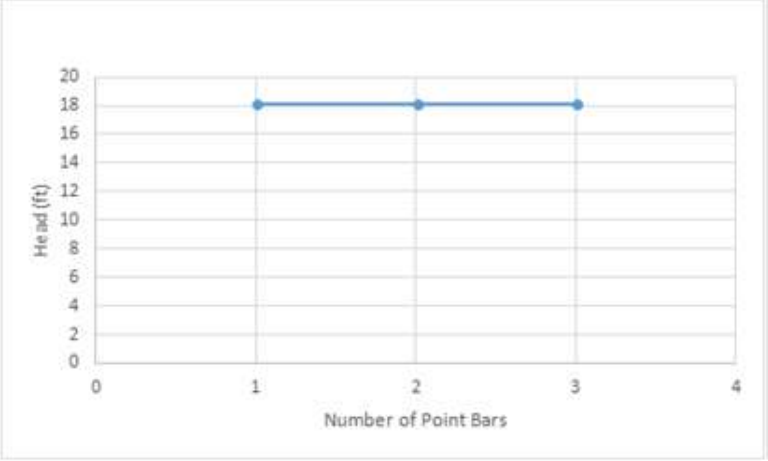

Fig. 20. The head calculated in each point bar at the landside levee toe in the case of several point bars within one levee alignment (a meander scroll) with a radius of 1300 feet and 180 degrees of curvature

to the results with 180 degrees of curvature. Very little difference was shown between the alignment with one point bar and the one with three point bars.

A levee alignment with 30 degrees of curvature was also analyzed, with much the samer results as the two previous analyses (presented in Fig. 22).

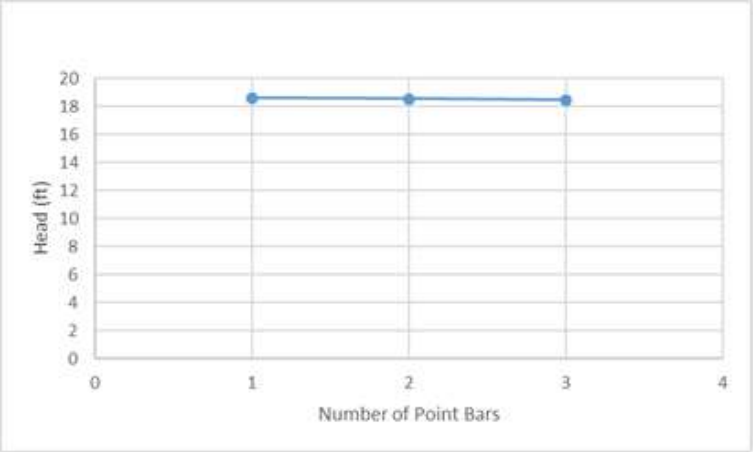

Fig. 21. The head calculated in each point bar at the landside levee toe in the case of several point bars within one levee alignment (a meander scroll) with a radius of 1300 feet and 90 degrees of curvature

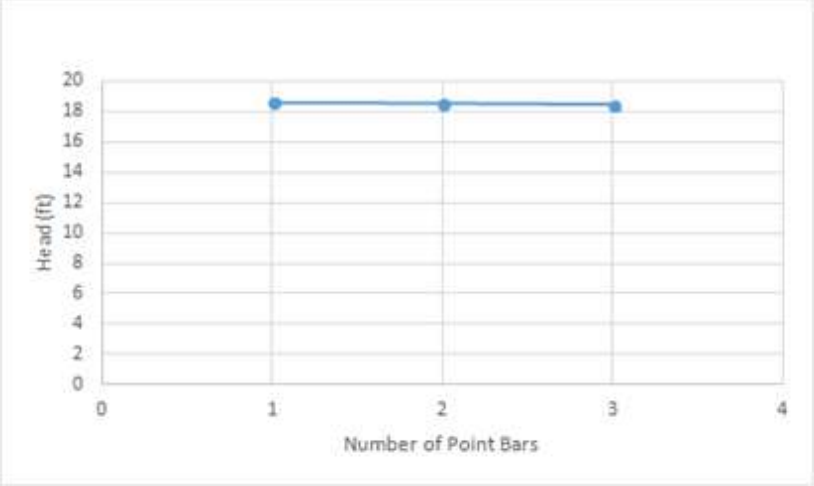

Fig. 22. The head calculated in each point bar at the landside levee toe in the case of several point bars within one levee alignment (a meander scroll) with a radius of 1300 feet and 30 degrees of curvature

The next model that was analyzed was the 180 degrees of curvature model, but with a smaller radius of 800 feet (see Fig. 23) to determine if radius would alter the effects of the existence of several point bars. The heads in the various scenarios again differed very little.

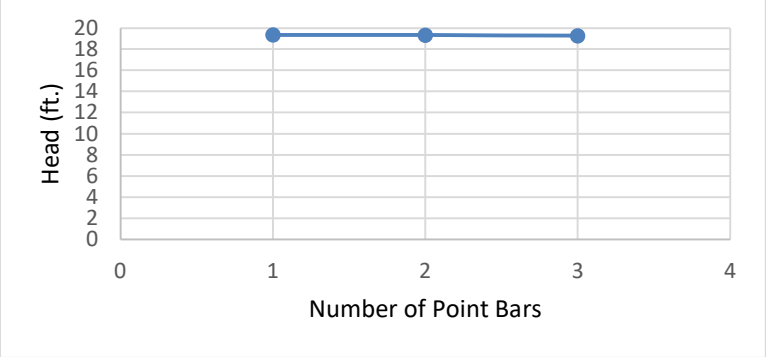

Fig. 23. The head calculated in each point bar at the landside levee toe in the case of several point bars within one levee alignment (a meander scroll) with a radius of 800 feet and 180 degrees of curvature

The last parameter that was changed to see if it would have an effect on the head in the point bars was the width of the clay drape (i.e. the thickness of the low-permeability zone between point bars). The thicker extreme of drape thickness was already used in the previous analyses, so two thinner drape widths were chosen (4 feet and 24 feet) to determine if the thickness of the clay drape would change the effects of multiple point bars on the heads found in the levee section. After calculating the heads in the point bars after changing the thickness of the clay drapes, it was demonstrated that the thickness of the drape also had very little effect on the head calculated in the point bars. The results are presented in Fig. 24.

Other geometric parameters were analyzed to determine the effects of the position of the point bar as it relates to the spatial arrangement of the levee alignment. Two geometric parameters were chosen to represent the relationship of the point bar to the

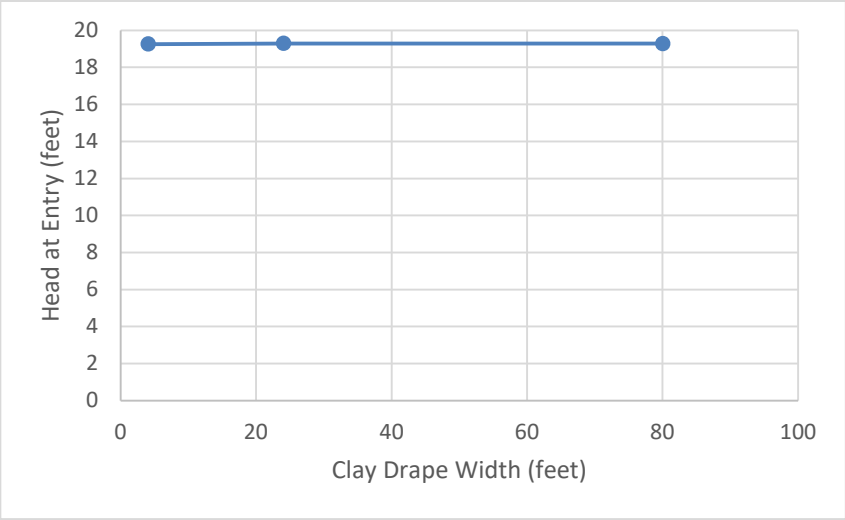

Fig. 24. A comparison of the head calculated at the landside levee toe in an alignment with three point bars, changing the thickness of the clay "drape" in between each subsequent point bar

levee alignment and are presented in Fig. 25. The lowercase “l” represents the perpendicular distance from the middle of the point bar to the front of the levee alignment. The uppercase “L” represents the total width of the point bar, measured from the widest points. These parameters were analyzed both independently and in conjunction to determine their effects and whether they were isolated effects or if the two parameters were related.

The parameters were first analyzed as a ratio, since if you keep the geometry of the levee section constant, you cannot change one without changing the other. However, maintaining a constant ratio of the two parameters produced an unexpected large change in head, which indicated that potentially one of the parameters had more of an effect on

the hydraulic head within the point bar. The results from maintaining the ratio of the two parameters constant are shown in Table 1.

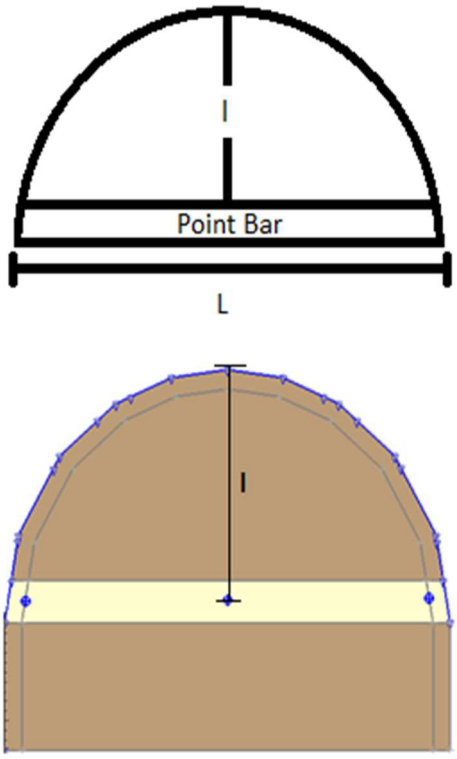

Fig. 25. Representations showing the "l" parameter, as well as the "L" parameter, two geometric parameters that relate the point bar to the levee alignment

Table 1. Results from experimenting with the “l” and “L” parameters while maintaining a constant ratio of the two

"l" (feet)	"L" (feet)	Ratio	Head at Entry (left, feet)	Head at Entry (right, feet)	Head at Middle (feet)
141	620	4.4	18.2	18.2	16.2
564	2480	4.4	17.5	17.8	6.2
		Difference	0.7	0.4	10

The difference between the two heads in the middle was, as previously mentioned, very large due to the fact that the distance that the water had to travel to get to the middle of the point bar was very large (1240 feet from any given direction) and therefore there were plenty of opportunities for leakage into the blanket, as opposed to the first case where the water only had to travel 310 feet to get to the middle of the point bar.

Next, each parameter was changed while maintaining the other parameter constant (therefore changing the ratio of the two). This was achieved by changing the radius of the levee alignment while maintaining one parameter constant and changing the other (i.e. changing the radius from 1300 to 2600 while keeping the "l" parameter at 150 feet will change the "L" parameter automatically, but change the ratio of the two). This investigation determined that both parameters had a significant effect on the head in the middle of the point bar, and that neither one affected the head at the levee toe significantly (which was expected since the distance that was traveled underneath the levee did not change in any of the cases since the levee width was held constant).

Isolating the parameters provided more unexpected results. When the length of the point bar ("L") was changed it affected the head significantly when the "l" value was kept constant. The results are presented in Table 2 and show that almost doubling the ratio of the two parameters by increasing the "L" value caused a significant change in head in the middle of the point bar, which was not expected. However, it was expected that the distance from the front of the levee alignment ("l") would affect the head significantly and, in fact, a very slight change in "l" did result in a moderate change in the head (see Table 3).

Table 2. Experimentation with the two geometric parameters "l" and "L", maintaining "l" constant and changing the ratio of the two

"L" (feet)	"l" (feet)	Ratio	Head at Entry (left, feet)	Head at Entry (right, feet)	Head at Middle (feet)
620	141	4.4	18.2	18.2	16.2
1127	141	8.0	18.4	18.3	14.9
		Difference	0.2	0.1	1.3

Table 3. Experimentation with the "l" parameter, changing it while keeping "L" constant

"L" (feet)	"l" (feet)	Ratio	Head at Entry (left, feet)	Head at Entry (right, feet)	Head at Middle (feet)
620	141	4.4	18.2	18.2	16.2
620	120	5.2	18.4	18.4	16.9
620	111	5.6	18.3	18.3	17.0
		Difference	0.2	0.2	0.8

Another aspect of the levee alignment that was analyzed was the effect of having an entirely curved levee section as opposed to having a section with a small curve and some straight levee sections adjacent to it (see Fig. 26 for illustration). This was accomplished by creating a completely curved model with a specific radius and running the three-dimensional finite element analysis program to calculate the heads in the middle and also on the sides, underneath the landside levee toe. Another model was created with the same degree of curvature, but only a fraction of the original radius was used, and then

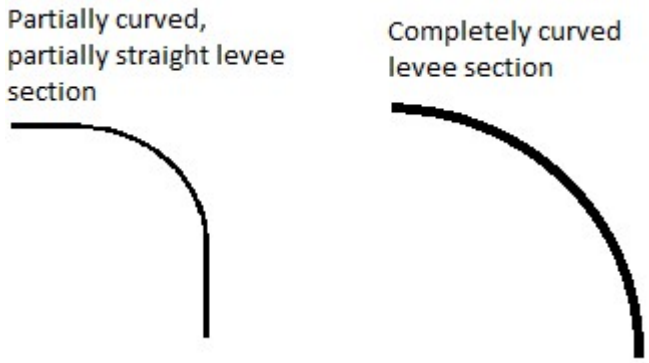

Fig. 26. Comparison of a completely curved levee section to a levee section with a portion curved and two straight levee sections on either side

the rest of the distance (so that the two models would terminate at close to the same point) was made up of linear levee sections. Both models were analyzed and it was determined that the head calculated in the center of the landside was practically the same in both models, but the head calculated at the levee toe was different. The head at the levee toe in the completely curved levee section was higher, most likely due to the concentration of head that occurs as a result of the curvature. The results are presented in Table 4.

Table 4. Effects of having an entirely curved levee section vs. partially curved and partially straight levee section

	Head at Toe (left, ft.)	Head at Toe (right, ft.)	Head at Middle (ft.)
Curved	18.7	18.6	14.5
Straight	18.1	18.1	14.4
Difference	0.6	0.5	0.1

Summary of Behavior

The parametric analysis identified parameters that characterize the behavior of underseepage through a point bar underneath a curved levee section. Fig. 13 demonstrates that landside point bar length does not have a large effect on the hydraulic head and shows that the critical location for hydraulic gradient is at the landside toe of the levee. Fig. 15 shows that angle of incidence of the point bar with the levee section has a variable effect on the hydraulic head. Fig. 16 shows that the hydraulic conductivity ratio of the blanket to the point bar can have a large effect on the hydraulic gradient and hydraulic head. Figs. 18 and 19 and Tables 1 through 4 show that the levee curvature affects the hydraulic head and is most critical at the landside toe of the levee. Figs. 20 through 23 show that the number of point bars does not have a significant effect on the hydraulic head underneath the levee toe, and Fig. 24 shows that the thickness of a clay drape between point bars also does not significantly affect the hydraulic head, which shows that a meander scroll can be treated as a point bar in analysis.

After comparing results from this parametric analysis with those found in Polanco Boulware (2017), it was determined that the parameters that make an abandoned channel and a point bar different do not significantly affect the calculations, as long as they are compared at the same type of levee section (either curved or straight). The levee curvature would also have the same effect on the hydraulic head whether an abandoned channel or a point bar was crossing the levee section. As a result, three combined parameters could be chosen to create the response surface sourced from the parametric analyses on the point bar and the abandoned channel. These parameters were chosen by

identifying the general behavior of the underseepage as a result of the presence of the point bar or abandoned channel crossing the levee alignment.

The first of these factors was the thickness of the blanket above the point bar. As was previously mentioned, the head did not increase dramatically with the inclusion of the point bar. However, the blanket thickness decreased significantly as a result of the low permeability blanket being replaced by the highly pervious point bar material. This increased the hydraulic exit gradient simply by reducing the length that the water had to travel to reach the surface. The reduction of blanket thickness also decreased the factor of safety with respect to heave. The thickness of the blanket above the point bar also affected the amount of leakage (a relationship between hydraulic conductivity and thickness of a layer, discussed in detail in the next section) that occurred. The thickness of the point bar was also determined as an important factor in calculating the modified leakage that affected the hydraulic head regime. The leakage was also affected by the ratio between hydraulic conductivities of the point bar and the blanket. As the blanket hydraulic conductivity approached the same value as the point bar hydraulic conductivity, the leakage increased and the head in the point bar therefore decreased.

The second factor that affected the factor of safety was a “tongue” of higher head that occurs in the point bar as a result of the concentration of flow within the point bar (see Fig. 27). The “tongue” refers to a difference in the position of a specific contour within the point bar as it relates to the position of the rest of the contour outside of the point bar when looking at head contours in plan view. When the contour enters the point bar, it moves forward from where it would have been if the blanket material that surrounds the point bar were totally homogeneous (i.e. if there were no point bar). This

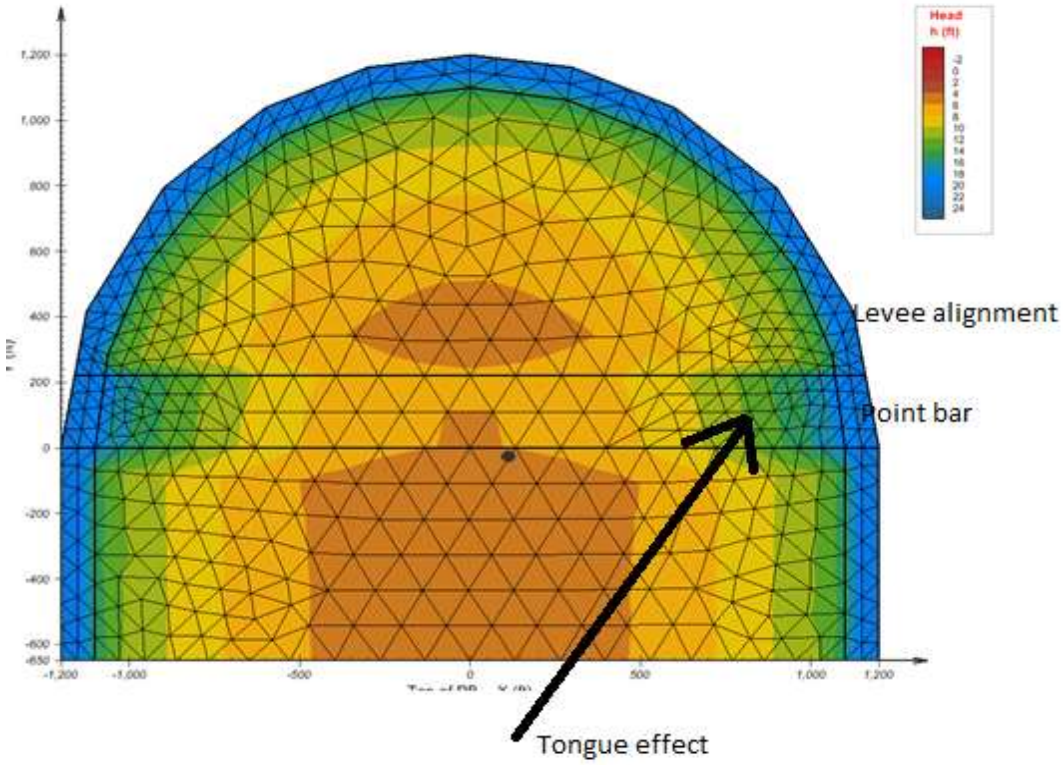

Fig. 27. A view of the "tongue effect" mesh and head contours generated by SVFlux within a levee with 180 degrees of curvature

phenomenon was caused by the ratio of hydraulic conductivities of the foundation material and the point bar material. As this ratio changed, the length of the "tongue" changed accordingly. The angle of incidence of the point bar also affected the location of the maximum head created by the tongue, and therefore was another parameter that was included in the development of the response surface.

The last factor that affected the factor of safety was the riverside length of the channel or point bar. This factor would generally have a more obvious effect in abandoned channels, but could affect the head regime with a point bar or meander scroll.

Curvature of the levee section also had an effect on the factor of safety, because it concentrated hydraulic head and also enhanced the hydraulic head in geomorphic features like point bars and abandoned channels. However, instead of including the curvature as part of the factors that characterized the flow in the levee alignment, it was proposed that the effects of curvature be superimposed in analysis after the development of the response surface, which was developed by Polanco Boulware (2017) and which will be described below.

Response Surface for a Straight Levee

After determining the parameters that affect the behavior of underseepage in the point bar, a response surface was created using these influential parameters. The response surface needed to be created to be able to run the Monte Carlo analysis, and the three parameters chosen needed to be so combined as to be able to calculate an accurate hydraulic head in any levee alignment with a point bar, regardless of its geometry or materials. Upon comparison with research done by Polanco Boulware (2017) on the effects of abandoned channels underneath a levee, it was determined that the point bar and abandoned channel could be represented by a single response surface representing both geomorphic features. The difference between the abandoned channel and the point bar analyses is that a factor will be included to account for the curvature of the levee, since point bars are generally found underneath curved levee sections as a result of their deposition, and abandoned channels can be found under either curved or linear levee alignments.

The first parameter in the response surface is a combined parameter describing the hydraulic head "tongue" effect caused by the difference in hydraulic conductivities of adjacent materials underneath the levee, as previously described. In the case of the point bar, the difference is caused by the higher hydraulic conductivity of the point bar, which is directly adjacent to a lower hydraulic conductivity blanket layer, causing more head loss. The angle of incidence can also change this effect, and therefore has been included in this combined parameter to fully describe this effect. The tongue effect, Tch, is therefore described by a combination of hydraulic conductivity parameters:

$$T_{ch} = \frac{K_{ch}}{K_f} \sin \alpha \tag{1}$$

where K_{ch} is the abandoned channel or point bar hydraulic conductivity, K_f is the foundation hydraulic conductivity, and α is the angle of incidence of the point bar with the levee alignment (see Fig. 28).

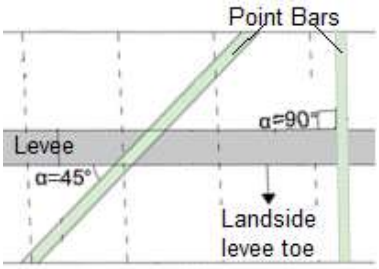

Fig. 28. Angle of incidence, α, for two point bars crossing a levee section, with values of α=45° and α=90°

The riverside blanket length was also determined to have an effect on the underseepage, especially in the analyses of the abandoned channel done by Polanco Boulware (2017). Therefore, this parameter was also chosen to be used in the response surface, with the modification that the blanket length is measured over the point bar, as opposed to a channel, as in Boulware's research. The chosen descriptor for this parameter is:

$$RL = Riverside\ Blanket\ Length\ over\ point\ bar \tag{2}$$

or Riverside Length, measured in feet.

The leakage that occurs between the foundation or geomorphic feature material and the blanket material was also determined to have a significant effect on the hydraulic head, so it was chosen as another parameter to be included in the response surface. The USACE defines leakage as a relationship between hydraulic conductivities and thicknesses of the layers in question, or in our case the foundation and the blanket (USACE 2005). The full parameter is defined as the modified leakage factor or:

$$\lambda_m = \sqrt{\frac{K_{ch} * t_b * t_{pb}}{K_b}} \tag{3}$$

where K_{ch} is the abandoned channel or point bar hydraulic conductivity, t_b is the thickness of the blanket, t_{pb} is the thickness of the point bar, and K_b is the hydraulic conductivity of the blanket.

Based on these parameters, a response surface was created that can be used for straight levee sections with abandoned channels, point bars, or meander scrolls present in the foundation. This response surface is represented by a family of curves, which are presented in Appendix A. This family of curves relates the three combined parameters to the maximum hydraulic head in the channel, point bar, or meander scroll feature. This response surface can be used to calculate the maximum hydraulic head for other levee alignments and rivers.

Effects of Levee Curvature

Beyond the effects of the response surface parameters, curvature of levee alignments also influences seepage underneath levees. As cited in Chapter 2, previous research by Sittinan Benjasupattananan has already established the effect of curvature on the hydraulic head on the landside of a levee (Benjasupattananan 2013) but did not concern itself with the presence of a point bar in a curved levee section. Benjasupattananan's research indicated that head increases significantly in the curved portion of the levee alignment (see Fig. 29). As part of our research, we created models to confirm the effects of curvature observed by Benjasupattananan (2013, see Appendix B), and then added onto those models to determine the effects of a point bar within a curved levee regime to establish whether a similar methodology could be used.

Our initial, confirmatory analyses were performed on a levee alignment with no point bar and 60 degrees of curvature (Dc), as shown in Fig. 30. Results are provided in Fig. 31 along with Benjasupattananan's results, and the results from this research confirm what was established by Benjasupattananan – the head at the landside toe of a levee

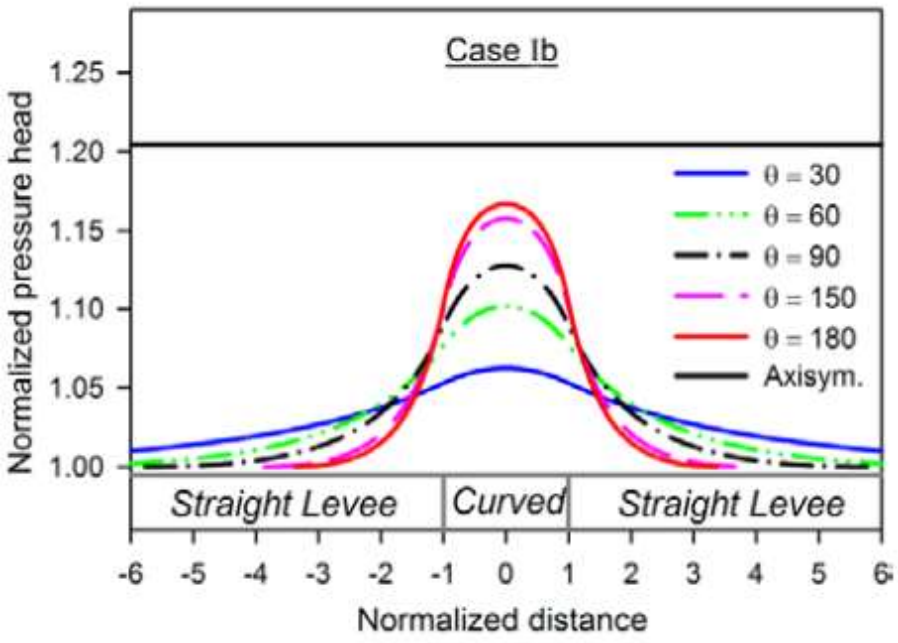

Fig. 29. Effect of levee curvature on pressure head, from Benjasupattananan (2013)

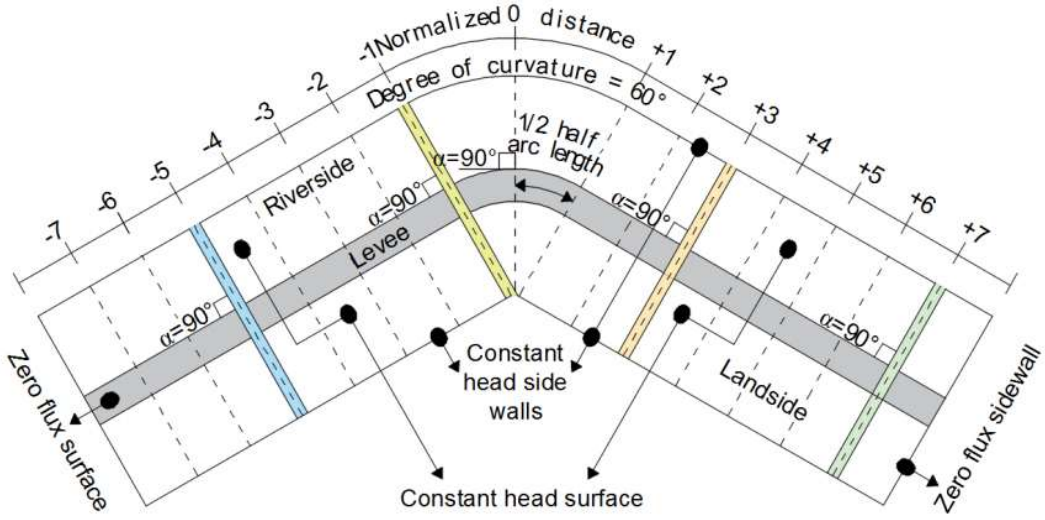

Fig. 30. Schematic plan view of the curvature model used for Dc = 60º and α = 90º showing channel features at ND = -5, -1, +3, +7

increases with increasing degrees of curvature. When point bars are introduced, the head increases at the landside toe of the levee, as seen in Fig. 31. After analyzing the existence

of the point bar within the curved levee alignment, preliminary results were plotted against the results of a curved levee without any point bar, to demonstrate the difference. The results are plotted normalized to the residual values calculated at a normalized radial distance of 8 (or in other words, normalized to a straight levee section).

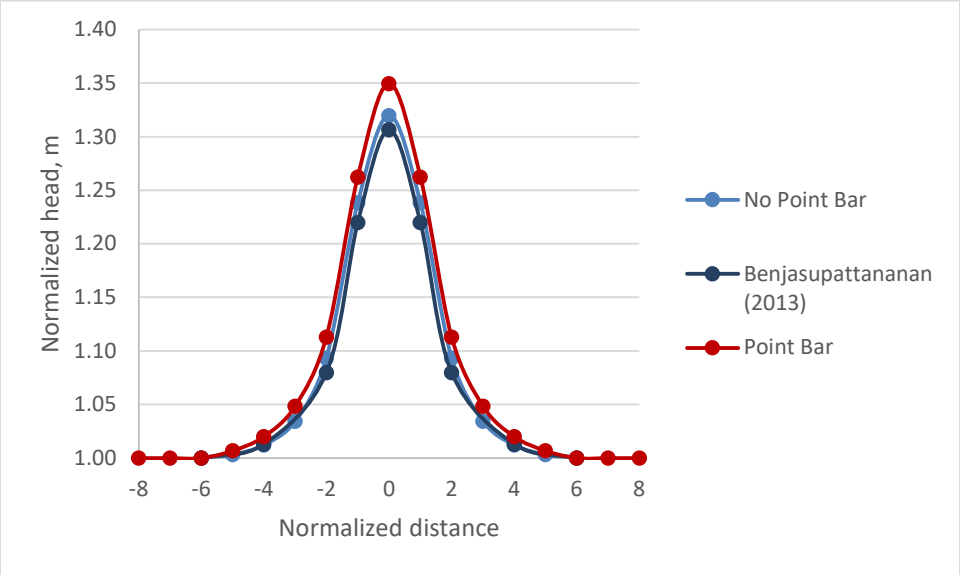

Fig. 31. Graph depicting the effect of curvature on head at the toe of a levee, with and without a point bar underneath. Dc = 60º and α = 90º, λ_m = 83.7, T_{ch} =1

Curvature Multiplier

After performing these initial analyses, several models were created, including models with 60, 90 and 150 degrees of curvature, Dc, and calculations were performed to analyze the effects of point bars with two angles of incidence (α), perpendicular (α = 90 degrees) to the levee alignment and at an angle of 45 degrees (α = 45 degrees). The angle of incidence of the point bar also has an obvious effect, which will be described subsequently. The models created for these analyses were created using the same parameters and boundary conditions as Benjasupattananan (2013), but also included a

point bar intersecting the levee alignment. A plan view of the 90 degrees of curvature model is presented in Fig. 32. The purpose of creating these models was to calculate curvature multipliers for various values of curvature, angle of incidence, modified leakage, and tongue effect. Once curvature multipliers have been established, these multipliers can be used on the response surface for a straight levee section to calculate the hydraulic head induced by a combination of geomorphic features and levee curvature.

Point bars were analyzed at different distances away from the curved portion of the levee, spaced at equal distances normalized to the arc length of the curve (ND). Analyses were performed on the several degrees of curvature and with point bars in different locations, and from these analyses a curvature response surface was generated to

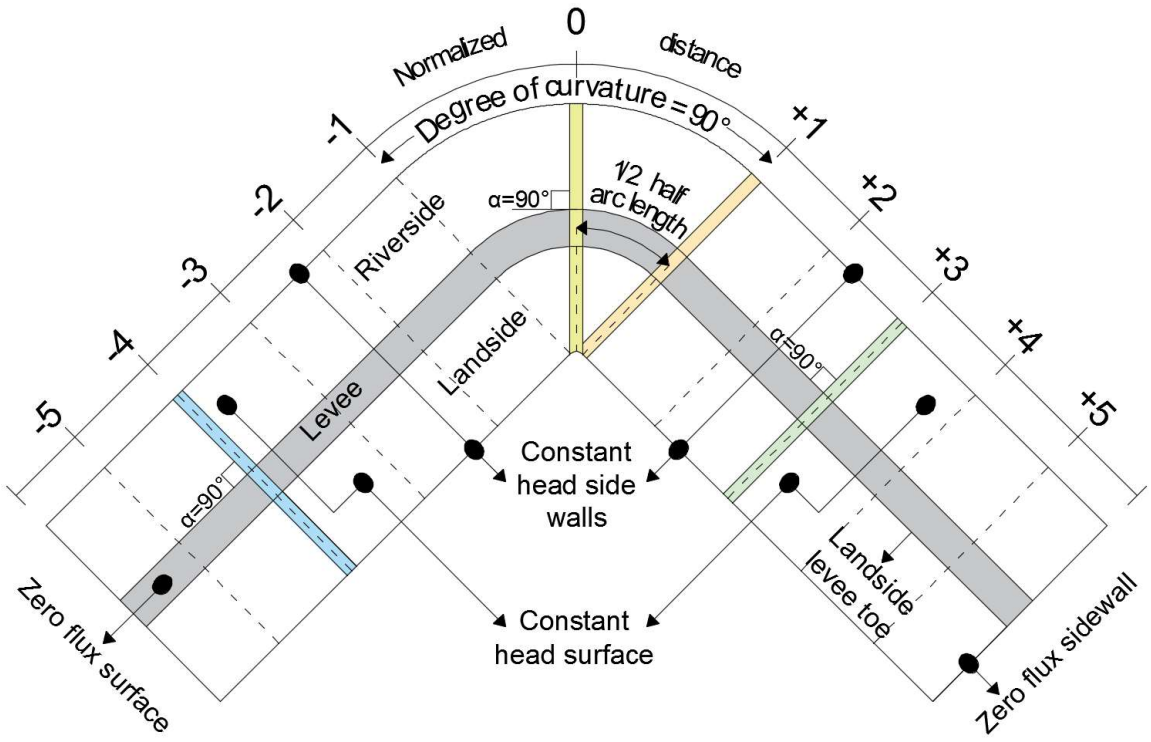

Fig. 32. Schematic plan view of the curvature model used for Dc = 90º and α = 90º showing point bar features at ND = -4, 0, +1 +3

be able to perform point bar analysis. Results of analyses that accompany Fig. 32 are presented in Fig. 33 and Table 5 below.

T_{ch} in Fig. 33 represents the "tongue effect" associated with the point bar. λ_m corresponds to the modified leakage factor. As seen in Fig. 33, different curvature multipliers result from the combination of different values of T_{ch} and λ_m. As λ_m increases, the head loss through the blanket layer decreases. As T_{ch} increases, the head loss will also

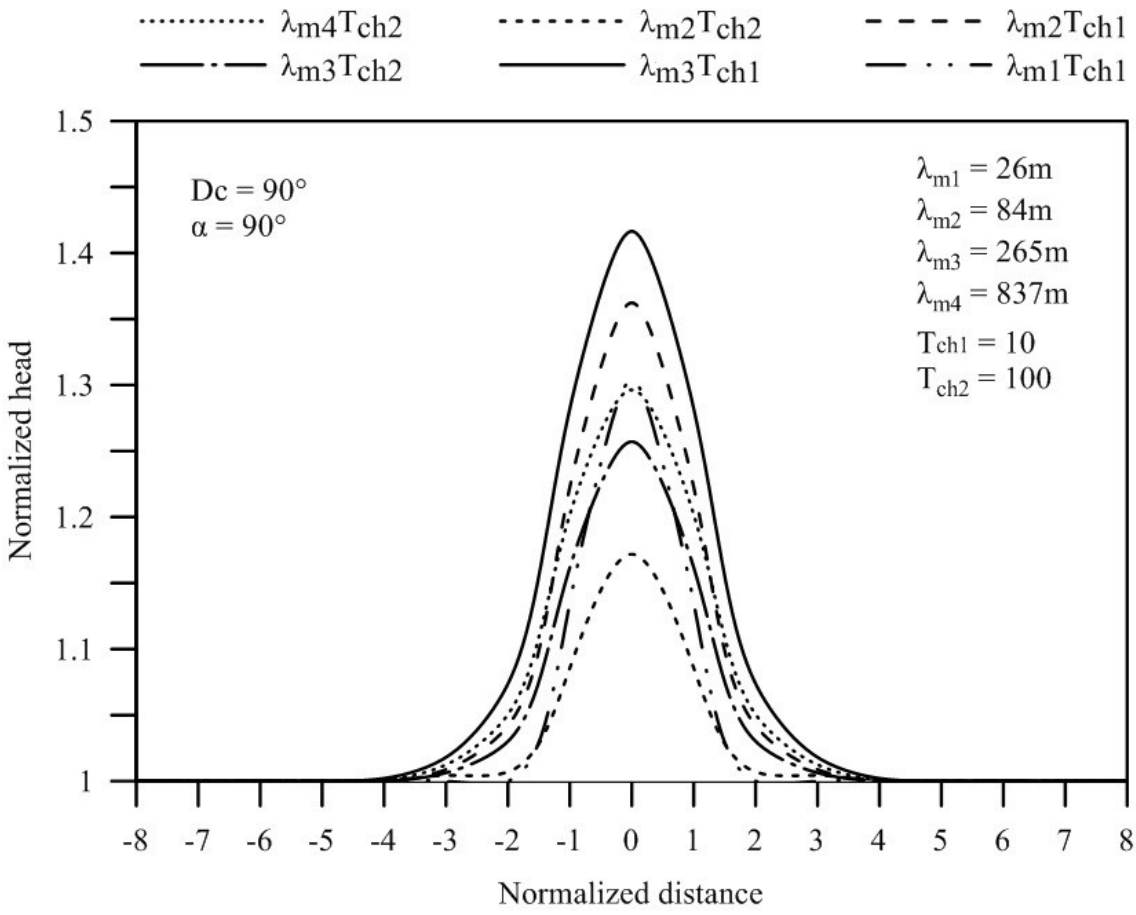

Fig. 33. Results for the curvature model with Dc = 90º and α = 90º

increase. Hence, the combination of a high λ_m (less head loss through the blanket) and a low T_{ch} (less head loss through the point bar) provides the highest coefficient (λ_{m3} T_{ch1}).

The combination of an average (high) modified leakage with a high tongue (λ_{m2} T_{ch2}) provides the smallest coefficient due to the fact that the leakage between the blanket and

Table 5. Parameters and results for the curvature model with Dc = 90º and α = 90º

Curvature multiplier for *Dc* = 90º with *α* = 90º						
K_f = 1E-05 m/s, t_b = 2 m, t_{ch} = 3.5 m, t_f = 32 m, w_{ch} = 10 m, RL = 200 m						
Stage	$\lambda_{m1}T_{ch1}$	$\lambda_{m2}T_{ch1}$	$\lambda_{m3}T_{ch1}$	$\lambda_{m2}T_{ch2}$	$\lambda_{m3}T_{ch2}$	$\lambda_{m4}T_{ch2}$
K_b (m/s)	1.00E-06	1.00E-07	1.00E-08	1.00E-06	1.00E-07	1.00E-08
K_{ch} (m/s)	1.00E-04	1.00E-04	1.00E-04	1.00E-03	1.00E-03	1.00E-03
λ_m (m)	26.5	83.7	264.6	83.7	264.6	836.7
T_{ch}	10	10	10	100	100	100
λ (m)	25.3	80.0	253.0	25.3	80.0	253.0
Normalized distance, ND	Head at top of channel (m)					
-8	1	1	1	1	1	1
-7	1	1	1	1	1	1
-6	1	1	1	1	1	1
-5	1	1	1	1	1	1
-4	1	1	1	1	1	1
-3	1.00	1.01	1.02	1.00	1.01	1.01
-2	1.00	1.04	1.07	1.01	1.03	1.05
-1	1.14	1.22	1.28	1.09	1.16	1.20
0	1.30	1.36	1.42	1.17	1.26	1.30
1	1.14	1.22	1.28	1.09	1.16	1.20
2	1.00	1.04	1.07	1.01	1.03	1.05
3	1.00	1.01	1.02	1.00	1.01	1.01
4	1	1	1	1	1	1
5	1	1	1	1	1	1
6	1	1	1	1	1	1
7	1	1	1	1	1	1
8	1	1	1	1	1	1

foundation layer (λ) is low, allowing for more dissipation through the blanket, contrary to the previous scenario where $\lambda \approx \lambda_m$. Finally, the combination of a low λ_m and T_{ch} (λ_{m1} T_{ch1}) provides an average coefficient where $\lambda \approx \lambda_m$. The results of these combinations

were contrary to what the authors had originally hypothesized, which was that the superimposition of a high conductivity point bar and levee curvature would increase the seepage significantly. The reason for the difference is that the the geometry of the intersection of the high conductivity point bar with the levee alignment allows more 3D dissipation of the hydraulic head, as can be seen in Table 5 in the scenarios where $T_{ch} = T_{ch2}$.

Another set of analyses was performed using a degree of curvature of 90 degrees but changing the angle of incidence of the point bar to 45 degrees. A plan view of this model can be seen in Fig. 34.

The results of these analyses generally demonstrated a similar trend to that shown

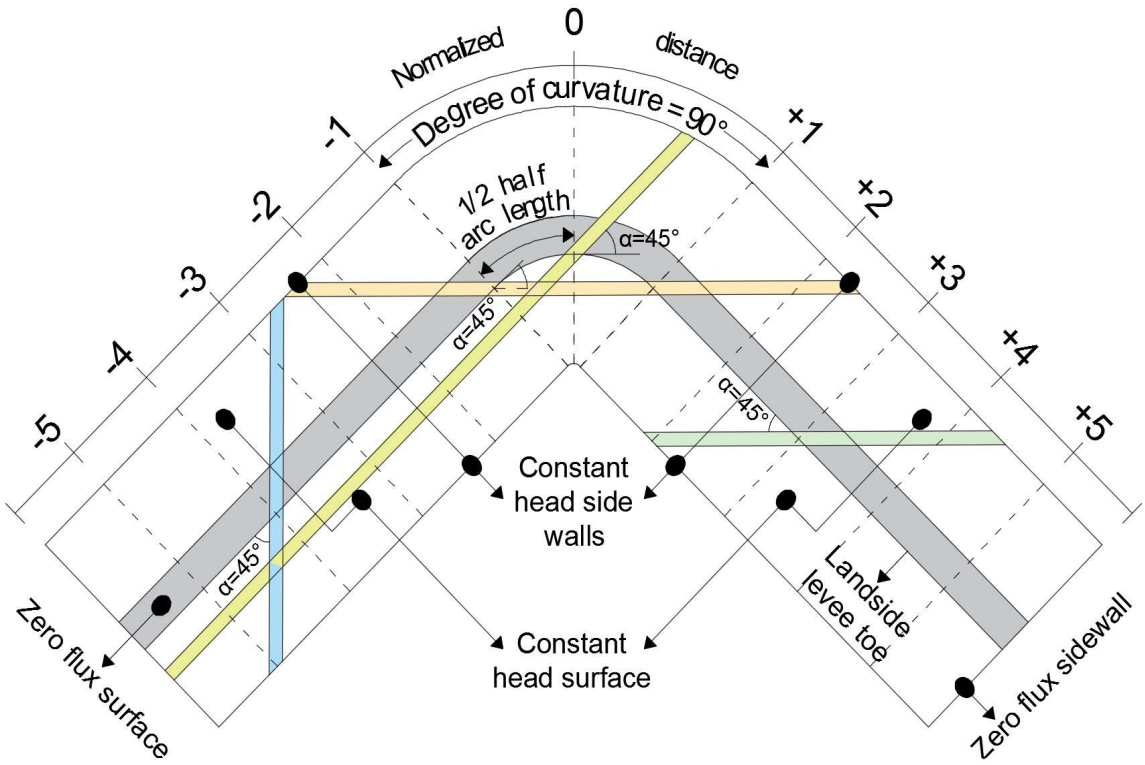

Fig. 34. Schematic plan view of the curvature model used for Dc = 90º and α = 45º showing point bar features at ND = -4, 0, +1 +3

by the analyses performed with the degree of curvature and angle of incidence of 90 degrees. However, two interesting differences were noted during the reduction of the data: first, the highest curvature coefficient is produced by the condition where both the tongue effect and the modified leakage factors are the lowest ($\lambda_{m1}T_{ch1}$), and second, the curves produced by analysis are not symmetrical (see Fig. 35). The curves were skewed due to the way that the point bar intersected with the levee, and the resultant location of the point bar in relation to the landside toe of the levee. Tabular results of the resultant curvature multipliers can be found in Table 6.

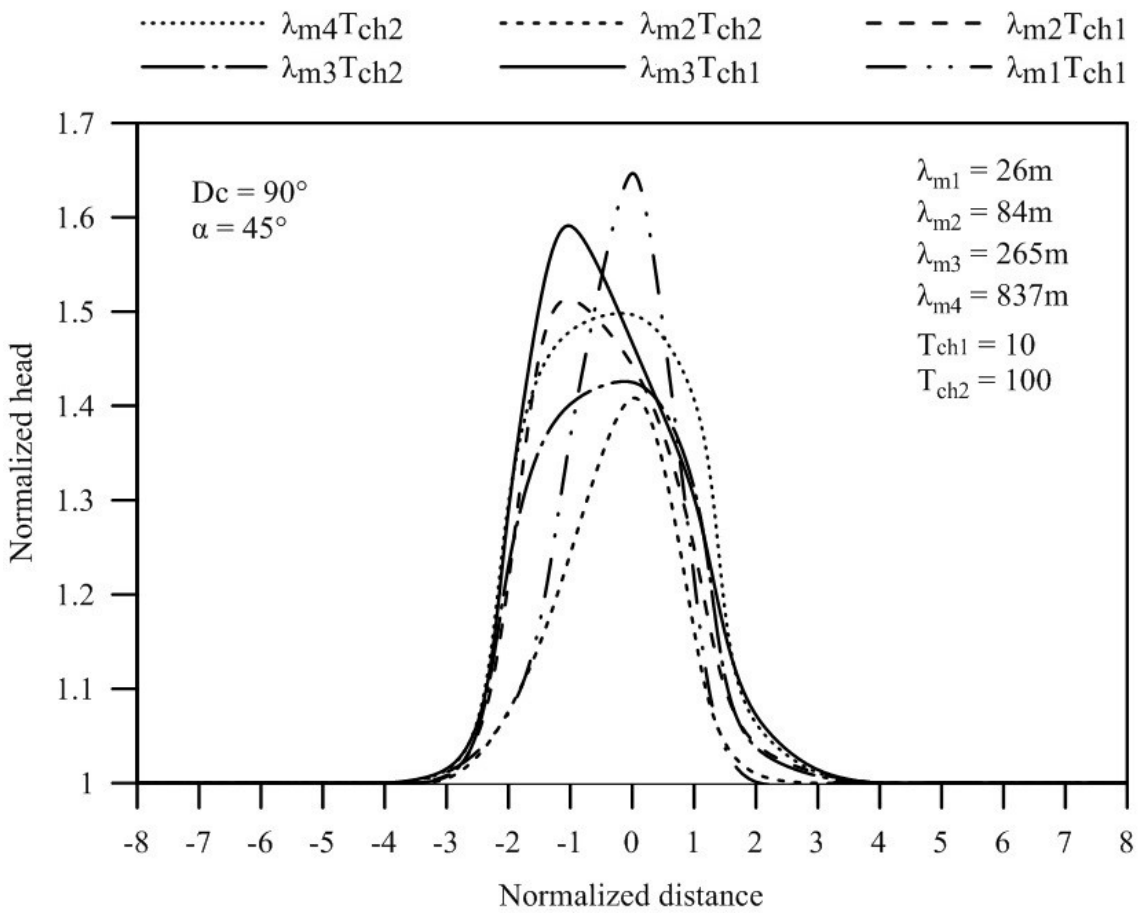

Fig. 35. Results for the curvature model with Dc = 90º and α = 45º

Table 6. Parameters and results for the curvature model with Dc = 90º and α = 45º

Curvature multiplier for *Dc* = 90º with *α* = 45º					
K_f = 1E-05 m/s, t_b = 2 m, t_{ch} = 3.5 m, t_f = 32 m, w_{ch} = 10 m, RL = 200 m					
Stage	$\lambda m_1 Tch_1$	$\lambda m_2 Tch_1$	$\lambda m_3 Tch_1$	$\lambda m_2 Tch_2$	$\lambda m_3 Tch_2$
Kb (m/s)	1.00E-06	1.00E-07	1.00E-08	1.00E-06	1.00E-07
Kch (m/s)	1.00E-04	1.00E-04	1.00E-04	1.00E-03	1.00E-03
λm (m)	26.5	83.7	264.6	83.7	264.6
Tch	10	10	10	100	100
λ (m)	83	262	830	83	262
Normalized distance, ND	Normalized head at top of channel				
-8	1	1	1	1	1
-7	1	1	1	1	1
-6	1	1	1	1	1
-5	1	1	1	1	1
-4	1	1	1	1	1
-3	1.01	1.01	1.02	1.00	1.01
-2	1.07	1.21	1.29	1.08	1.23
-1	1.37	1.51	1.59	1.24	1.40
0	1.65	1.44	1.47	1.41	1.43
1	1.22	1.25	1.30	1.16	1.31
2	1.00	1.04	1.07	1.00	1.04
3	1.02	1.01	1.01	1.01	1.01
4	1	1	1	1	1
5	1	1	1	1	1
6	1	1	1	1	1
7	1	1	1	1	1
8	1	1	1	1	1

The same type of analysis was performed using a degree of curvature of 150 degrees, and an angle of incidence of the point bar of 90 degrees. A plan view of this model can be seen in Fig. 36. The results of these analyses (see Fig. 37) generally demonstrated a similar trend to that shown by the analyses performed with the degree of curvature and angle of incidence of 90 degrees. The magnitudes of the normalized head

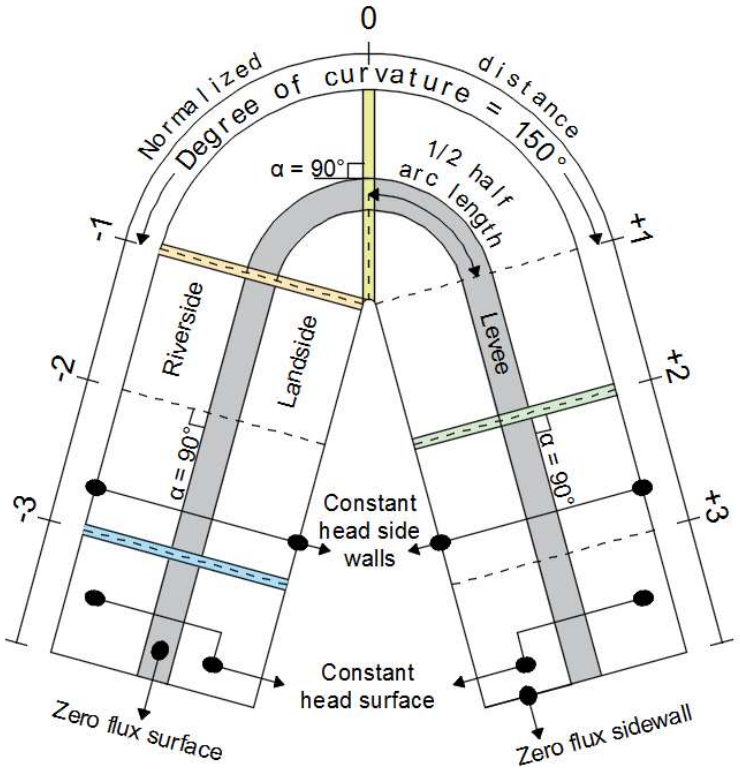

Fig. 36. Schematic plan view of the curvature model used for Dc = 150º and α = 90º showing point bar features at ND = -3, -1, 0 +2

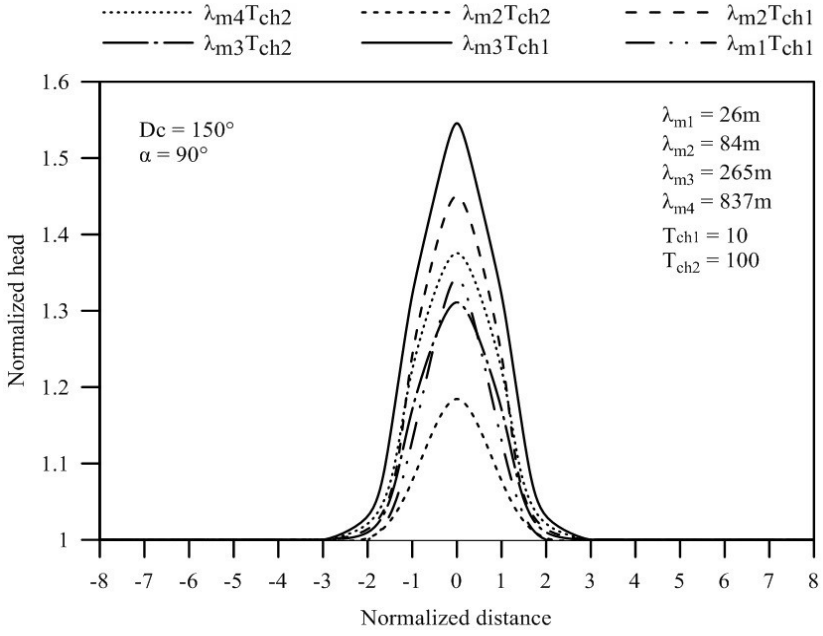

Fig. 37. Results for the curvature model with Dc = 150º and α = 90º

were noted to be larger than those reported from the model with 90 degrees of curvature (see Fig. 37), as was expected based on our prior research on the effects of the degree of curvature. Tabular results of the resultant curvature multipliers can be found in Table 7.

Table 7. Parameters and results for the curvature model with Dc = 150º and α = 90º

Curvature multiplier for *Dc* = 150º with *α* = 90º					
K_f = 1E-05 m/s, t_b = 2 m, t_{ch} = 3.5 m, t_f = 32 m, w_{ch} = 10 m, *RL* = 200 m					
Stage	$\lambda m_1 Tch_1$	$\lambda m_2 Tch_1$	$\lambda m_3 Tch_1$	$\lambda m_2 Tch_2$	$\lambda m_3 Tch_2$
K_b (m/s)	1.00E-06	1.00E-07	1.00E-08	1.00E-06	1.00E-07
K_{ch} (m/s)	1.00E-04	1.00E-04	1.00E-04	1.00E-03	1.00E-03
λ_m (m)	26.5	83.7	264.6	83.7	264.6
T_{ch}	10	10	10	100	100
λ (m)	83	262	830	83	262
Normalized distance, ND	Head at top of channel (m)				
-8	1	1	1	1	1
-7	1	1	1	1	1
-6	1	1	1	1	1
-5	1	1	1	1	1
-4	1	1	1	1	1
-3	1.00	1.00	1.00	1.00	1.00
-2	1.00	1.01	1.03	1.00	1.01
-1	1.13	1.24	1.32	1.08	1.17
0	1.34	1.45	1.55	1.18	1.31
1	1.13	1.24	1.32	1.08	1.17
2	1.00	1.01	1.03	1.00	1.01
3	1.00	1.00	1.00	1.00	1.00
4	1	1	1	1	1
5	1	1	1	1	1
6	1	1	1	1	1
7	1	1	1	1	1
8	1	1	1	1	1

An additional analysis was performed using a degree of curvature of 150 degrees, and an angle of incidence of the point bar of 45 degrees. A plan view of this model can be seen in Fig. 38.

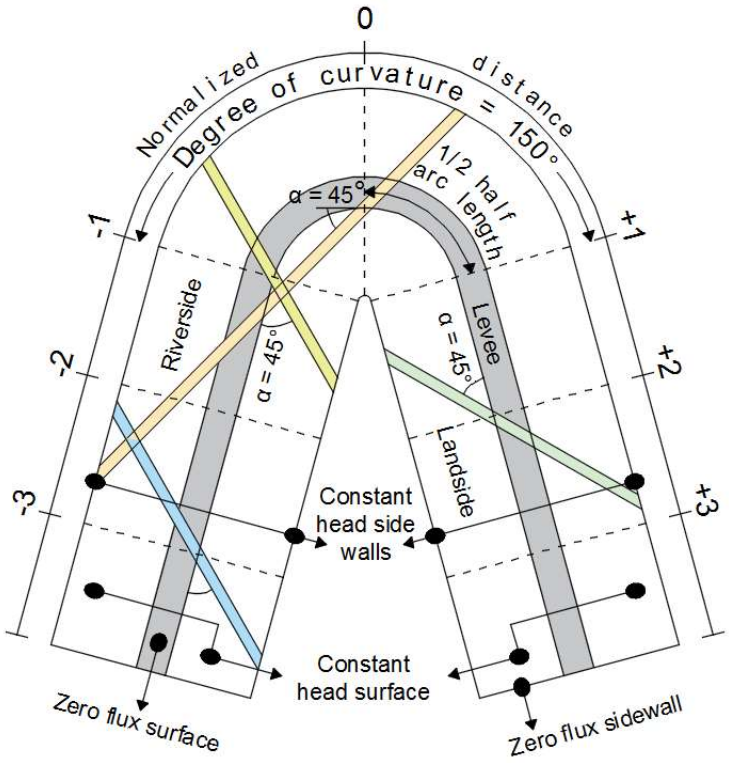

Fig. 38. Schematic plan view of the curvature model used for Dc = 150º and α = 45º showing channel features at ND = -3, -1, 0, +2

The results of these analyses generally demonstrated a similar trend to that shown by the analyses performed with the degree of curvature of 90 degrees and angle of incidence of 45 degrees. The same asymmetry was noted in the results, and the highest curvature coefficient was again calculated when the modified leakage and tongue effect factors were lowest (see Fig. 39). Again, it is our opinion that the geometry of the intersection of point bar with levee created this skew in the data. Tabular results of the resultant curvature multipliers can be found in Table 8.

The same type of analysis was performed using a degree of curvature of 60 degrees, and an angle of incidence of the point bar of 90 degrees. A plan view of this model was presented in the previous section and can be seen in Fig. 30.

Table 8. Parameters and results for the curvature model with Dc = 150º and α = 45º

Curvature multiplier for *Dc* = 150º with *α* = 45º					
K_f = 1E-05 m/s, t_b = 2 m, t_{ch} = 3.5 m, t_f = 32 m, w_{ch} = 10 m, *RL* = 200 m					
Stage	$\lambda m_1 Tch_1$	$\lambda m_2 Tch_1$	$\lambda m_3 Tch_1$	$\lambda m_2 Tch_2$	$\lambda m_3 Tch_2$
K_b (m/s)	1.00E-06	1.00E-07	1.00E-08	1.00E-06	1.00E-07
K_{ch} (m/s)	1.00E-04	1.00E-04	1.00E-04	1.00E-03	1.00E-03
λ_m (m)	26.5	83.7	264.6	83.7	264.6
T_{ch}	10	10	10	100	100
λ (m)	83	262	830	83	262
Normalized distance	Head at top of channel (m)				
-8	1	1	1	1	1
-7	1	1	1	1	1
-6	1	1	1	1	1
-5	1	1	1	1	1
-4	1	1	1	1	1
-3	1.00	1.00	1.00	1.00	1.00
-2	1.00	1.01	1.03	1.00	1.01
-1	1.24	1.27	1.33	1.16	1.22
0	1.72	1.56	1.64	1.48	1.56
1	1.21	1.27	1.35	1.15	1.35
2	1.10	1.11	1.05	1.04	1.08
3	1.05	1.08	1.01	1.02	1.04
4	1.05	1.08	1.01	1.02	1.04
5	1.05	1.08	1.01	1.02	1.04
6	1.05	1.08	1.01	1.02	1.04
7	1.05	1.08	1.01	1.02	1.04
8	1.05	1.08	1.01	1.02	1.04

The results of these analyses generally demonstrated a similar trend to that shown by the analyses performed with the degrees of curvature equal to 90 and 150 degrees, and angle of incidence of 90 degrees (see Fig. 40). One exception was demonstrated in the curve with the lowest modified leakage and lowest tongue effect factor (λm1Tch1). This analysis resulted in a high peak which may be in part due to the low ratios of hydraulic conductivity between the blanket, point bar, and foundation. This low permeability ratio

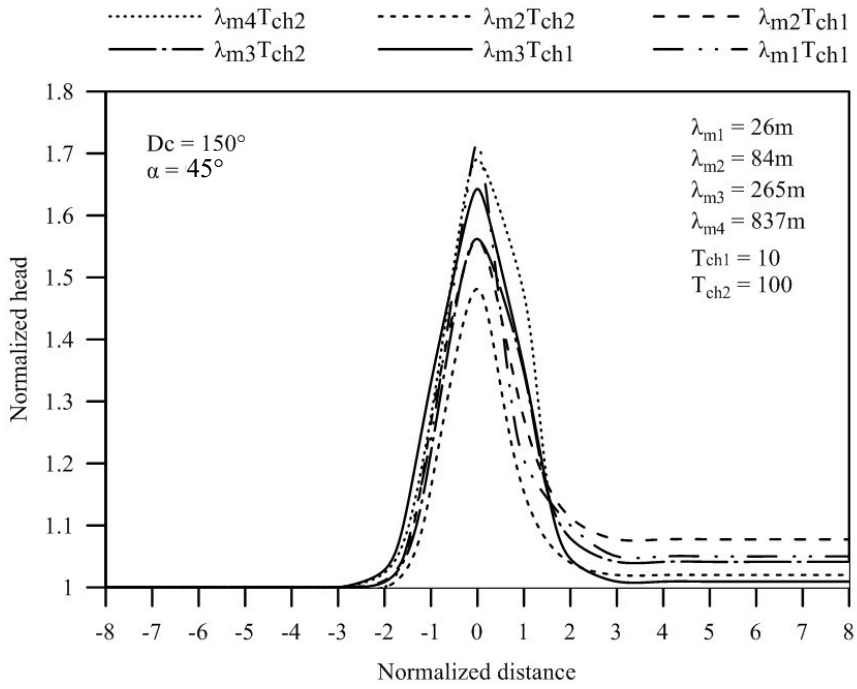

Fig. 39. Results for the curvature model with Dc = 150º and α = 45º

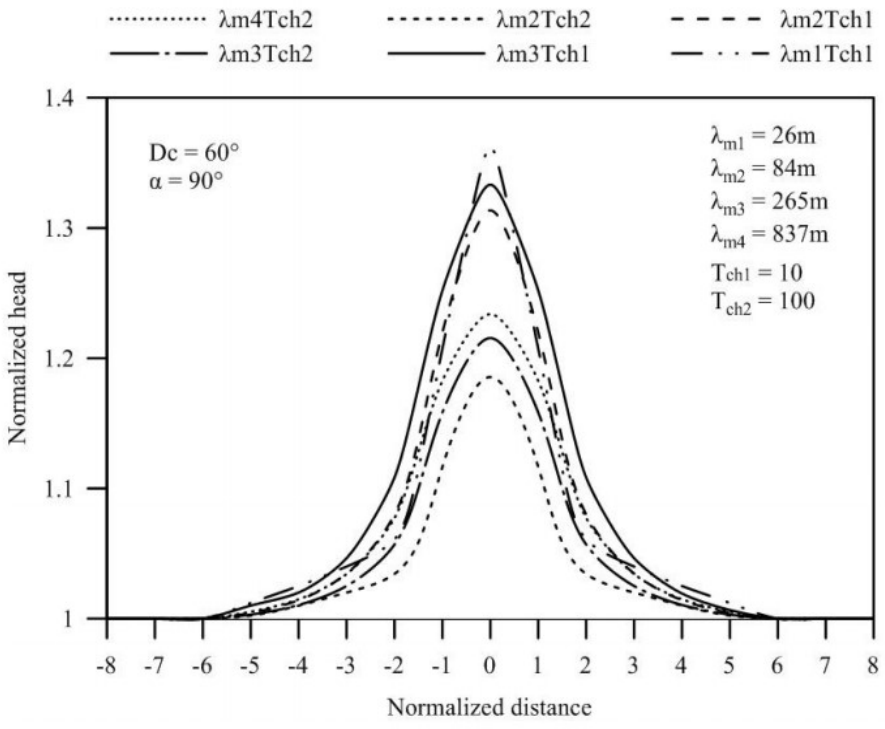

Fig. 40. Results for the curvature model with Dc = 60º and α = 90º

could have caused the seepage to have been distributed more evenly throughout all of the materials, which could have changed the results at the middle disproportionately in the case of the 60 degrees of curvature model because of the relatively lower degree of curvature. It should also be noted that the results of these analyses have been normalized to the results of a straight levee without a channel, and that the peaks indicate an increased change from straight levee results without a channel and not necessarily a net increase in the actual value. The magnitudes of the normalized head were noted to be comparable to but generally slightly less than those reported from the model with 90 degrees of curvature, as was expected based on our prior research on the effects of the degree of curvature. Tabular results of the resultant curvature multipliers can be found in Table 9.

The final analysis performed used a degree of curvature of 60 degrees, and an angle of incidence of the point bar of 45 degrees. A plan view of this model can be seen in Fig. 41.

The results of these analyses generally demonstrated a similar trend to that shown by the analyses performed with the degree of curvature of 90 degrees and angle of incidence of 45 degrees, except that the peaks were smaller. Similar, but more pronounced asymmetry was noted in the results. The highest curvature coefficient was calculated when the modified leakage and tongue effect factors were highest (see Fig. 42) but were not significantly different than the curvature coefficient calculated when modified leakage and tongue effect factors were lowest. The highest curvature coefficient being associated with the highest modified leakage and tongue effect factors may be due to the angle of incidence being so close to the degree of curvature. It is our opinion that

Table 9. Parameters and results for the curvature model with Dc = 60º and α = 90º

Curvature multiplier for *Dc* = 60º with *α* = 90º						
K_f = 1E-05 m/s, t_b = 2 m, t_{ch} = 3.5 m, t_f = 32 m, w_{ch} = 10 m, RL = 200 m						
Stage	$\lambda_{m1}T_{ch1}$	$\lambda_{m2}T_{ch1}$	$\lambda_{m3}T_{ch1}$	$\lambda_{m2}T_{ch2}$	$\lambda_{m3}T_{ch2}$	$\lambda_{m4}T_{ch2}$
K_b (m/s)	1.00E-06	1.00E-07	1.00E-08	1.00E-06	1.00E-07	1.00E-08
K_{ch} (m/s)	1.00E-04	1.00E-04	1.00E-04	1.00E-03	1.00E-03	1.00E-03
λ_m (m)	26.5	83.7	264.6	83.7	264.6	836.7
T_{ch}	10	10	10	100	100	100
λ (m)	25.3	80.0	253.0	25.3	80.0	253.0
Normalized distance	Head at top of channel (m)					
-8	1	1	1	1	1	1
-7	1	1	1	1	1	1
-6	1	1	1	1	1	1
-5	1	1	1	1	1	1
-4	1.03	1.01	1.02	1.01	1.01	1.01
-3	1.04	1.03	1.05	1.02	1.03	1.03
-2	1.06	1.08	1.11	1.03	1.06	1.08
-1	1.21	1.22	1.25	1.12	1.16	1.18
0	1.36	1.31	1.33	1.19	1.22	1.23
1	1.21	1.22	1.25	1.12	1.16	1.18
2	1.06	1.08	1.11	1.03	1.06	1.08
3	1.04	1.03	1.05	1.02	1.03	1.03
4	1.03	1.01	1.02	1.01	1.01	1.01
5	1	1	1	1	1	1
6	1	1	1	1	1	1
7	1	1	1	1	1	1
8	1	1	1	1	1	1

the geometry of the intersection of point bar with levee created this skew in the data. Tabular results of the resultant curvature multipliers can be found in Table 10.

The analyses with an angle of incidence of 45 degrees resulted in variable skew amongst the three degrees of curvature analyzed. The skew from these analyses was definitely affected by the geometry of intersection of the point bars with the levees, but could also have been affected by the low tongue effect, which is indicative of a reduced hydraulic conductivity in the channel when compared to the surrounding area. The skew

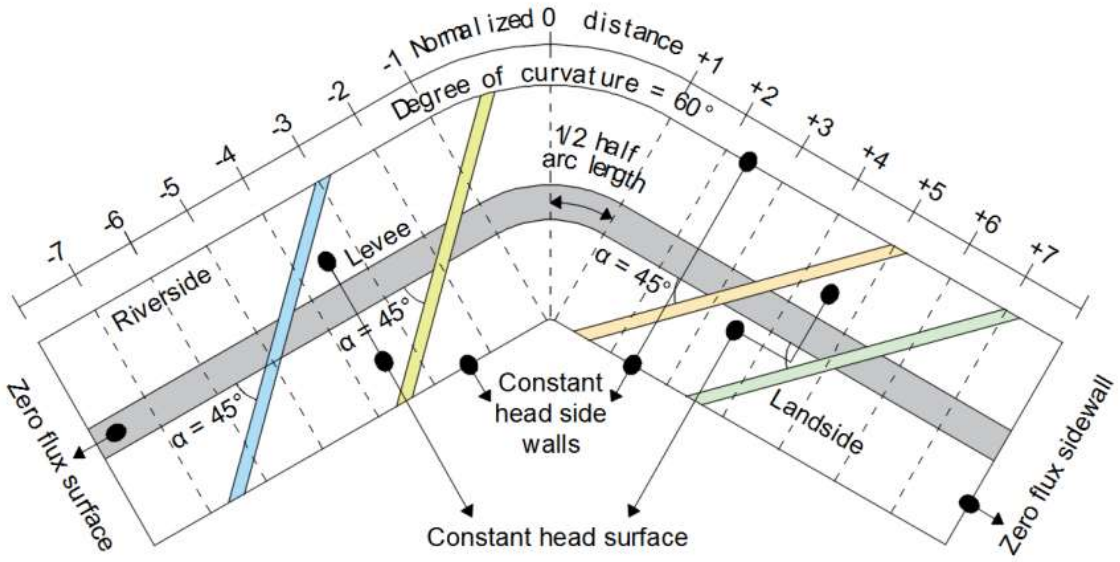

Fig. 41. Schematic top view of the curvature model used for Dc = 60º and α = 45º showing channel features at ND = -5, -2, +3, +5

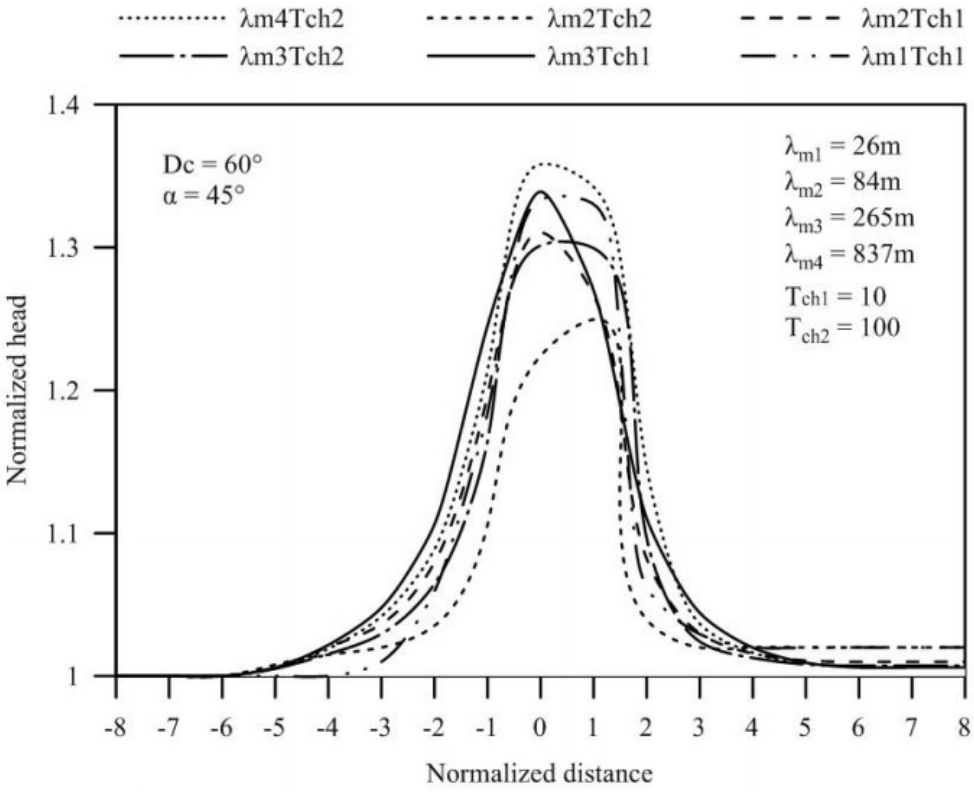

Fig. 42. Results for the curvature model with Dc = 60º and α = 45º

of the curves is also accompanied by changes in the magnitude of the peaks in the curves degrees of curvature include significant skew, with peaks occurring between in all three analyses. The analysis of the 150 degrees of curvature indicates peaks that are generally clustered around a normalized distance of 0, but the analyses of 90 and 60 degrees of curvature peaked at normalized distances between -2 and 2. No correlation was observed between the degree of curvature and magnitude of skew. Although the analysis of 150 degrees of curvature appeared to have generally more clustered peaks, it still

Table 10. Parameters and results for the curvature model with Dc = 60º and α = 45º

Curvature multiplier for *Dc* = 60º with *α* = 45º						
K_f = 1E-05 m/s, t_b = 2 m, t_{ch} = 3.5 m, t_f = 32 m, w_{ch} = 10 m, RL = 200 m						
Stage	λm_1 Tch_1	λm_2 Tch_1	λm_3 Tch_1	λm_2 Tch_2	λm_3 Tch_2	$\lambda_{m4}T_{ch2}$
K_b (m/s)	1.00E-06	1.00E-07	1.00E-08	1.00E-06	1.00E-07	1.00E-08
K_{ch} (m/s)	1.00E-04	1.00E-04	1.00E-04	1.00E-03	1.00E-03	1.00E-03
λ_m (m)	26.5	83.7	264.6	83.7	264.6	836.7
T_{ch}	10	10	10	100	100	100
λ (m)	25.3	80.0	253.0	25.3	80.0	253.0
Normalized distance	Head at top of channel (m)					
-8	1	1	1	1	1	1
-7	1	1	1	1	1	1
-6	1	1	1	1	1	1
-5	1	1	1	1	1	1
-4	1	1	1	1.02	1	1
-3	1.01	1.04	1.05	1.02	1.03	1.04
-2	1.06	1.08	1.11	1.04	1.06	1.09
-1	1.18	1.20	1.25	1.11	1.16	1.21
0	1.33	1.31	1.34	1.22	1.30	1.36
1	1.33	1.27	1.27	1.25	1.30	1.34
2	1.06	1.08	1.11	1.04	1.10	1.15
3	1.03	1.03	1.04	1.02	1.02	1.04
4	1.02	1.02	1.02	1.02	1.01	1.02
5	1.02	1.01	1.01	1.02	1.01	1.01
6	1.02	1.01	1.01	1.02	1.01	1.00
7	1.02	1.01	1.01	1.02	1.01	1.00
8	1	1.01	1.01	1.02	1.01	1.00

demonstrated skew in the normalized head that did not return to a value of 1 as normalized distance increased.

CHAPTER 5

CONCLUSION

When modeling levees with uncertain or irregular foundations, current analysis methods tend to not fully characterize subsurface processes. It is difficult, with analysis methods such as the Blanket Theory to include complicated subsurface geometries like those found in areas with geomorphic features like buried point bars, abandoned channels, and meander scrolls. A new analysis method, proposed by Rice and Polanco (2012) and Polanco and Rice (2014) can account for uncertainties in levee foundations, and the purpose of this research was to supplement the development of this method for levees with a point bar, abandoned channel, or meander scroll connected to the foundation.

A point bar is a geomorphic feature that develops as the result of deposition on the inside bank of a curved section of a river. Sandy soils are normally deposited on this inside bank as the velocity of the water slows around this curve and the resulting bars form gradually. Over time, the river will often migrate away from these point bars and bury them in lower permeability overbank sediment that then becomes the foundation for man-made levees. Meander scrolls are a series of point bars separated by thin layers of low permeability sediment. Abandoned channels either form when tributaries or the main channel change course and abandon their original channels. All of these geomorphic features can concentrate the flow underneath a levee and effectively decrease the thickness of the blanket layer, resulting in a higher probability of levee failure due to heave.

To model the effects of point bars and meander scrolls in the foundations of curved levee sections, the finite element analysis program SVFlux (SoilVision, 2014) was used. A general model was created based on empirical data of the dimensions and characteristics of the three geomorphic features, and then modified to account for a wide range of geometries and physical features. Some of the geometric parameters included in the analysis were the radius of curvature of the curved levee alignment, as well as the degree of curvature, the length of the point bar, the angle of incidence of the point bar into the levee alignment, the number of and distance between point bars in the case of a meander scroll, as well as the horizontal distance from the front of the levee alignment to the middle of the point bar ("l") and the length of the point bar as it traverses the entire width of the levee alignment ("L"). The hydraulic conductivity of and the hydraulic conductivity ratio between blanket and point bar were also analyzed to determine their effects on the underseepage through geomorphic features.

After determining the effects of many different physical parameters, as well as the general behavior of underseepage in point bars within the context of levee foundations, the most important parameters were chosen and combined into three parameters representative of the behavior in these geomorphic features. A response surface, or simplified mathematical model, for a straight levee with an intersecting point bar was created using these three combined parameters to be used for the Monte Carlo simulation. After creating the response surface, its results were compared with results from a series of finite element models using the same parameter values. This comparison was performed to determine if the response surface was accurately representing the underseepage behavior.

Because point bars are generally found near curved levee sections, it was also necessary to assess how curvature affected the response surface. To assess the effect of curvature, a series of finite element models were created with curvature and intersecting point bars. Three main degrees of curvature (60, 90, and 150 degrees), and two angles of point bar-levee intersection (45 and 90) were selected for analysis. In general, hydraulic head increased with increasing degree of curvature, because of the increased flow concentration. The angle of intersection tended to accentuate this effect, as increasing obliquity of intersection angle also caused increased hydraulic head measured at the landside toe of the levee. The angle of intersection also caused some unexpected effects, especially a skew of the location of the highest normalized head. The analyses of the 90 degree angle of intersection resulted in a predictable peak at the middle of the curved levee alignment, while the analyses of 45 the degree angle of intersection generally resulted in peaks away from the middle of the levee alignment. This skew is isolated to the analyses of the 45 degree angle of incidence, which indicates that the skew is a result of the geometry of the intersection of the point bar with the levee alignment. The angle of intersection was incorporated into the original response surface as part of one of the combined parameters previously mentioned. The degree of curvature was found to create a predictable effect, and so a series of multipliers for levee curvature were created. These multipliers are separate from the response surface, but are meant to be applied to the head calculated using the response surface for a resultant head that incorporates effects of point bar underseepage and levee curvature.

This method for use with point bars cannot be compared to other current methods because other current methods (like the USACE Blanket Theory equations) cannot

account for nonuniform foundation geometries. This is one of the obvious advantages of the Response Surface-Monte Carlo method - it can be used where other methods would need to overly simplify the foundation geometry and therefore calculate a possibly inaccurate factor of safety. A disadvantage of this specific paper's research is its lack of versatility as it can only be used for cases where the geomorphology contains a point bar or meander scroll or abandoned channel, however this shortcoming is to be remedied by subsequent research within the larger project, where several other geomorphic features will be studied and modeled to be able to apply this same Response Surface-Monte Carlo method.

REFERENCES

Allen, J.R. 1970. Physical processes of sedimentation, George Allen and Unwin, London.

Benjasupattananan, S. 2013. Deterministic and probabilistic approaches for modeling levee underseepage. Ph.D. dissertation, Univ. of Delaware, Newark, DE.

Duncan, M.J. 2000. Factors of safety and reliability in geotechnical engineering. Journal of Geotechnical and Geoenvironmental Engineering. ASCE 1264:307-316.

Gagliano, S. M., and van Beek, J. L. 1970. Geologic and geomorphic aspects of deltaic processes, Mississippi delta system. Hydrologic and geologic studies of coastal Louisiana. Vol. 1. Coastal Studies Institute, Louisiana State University, Baton Rouge.

Glynn, M.E. and Kuszmaul, Joel. 2010. Prediction of Piping Erosion along Middle Mississippi River Levees-An Empirical Model. USACE, Technologies and Operational Innovations for Urban Watershed Networks Research Program, ERDC/GSL TR-04-12. Originally published in 2004 and revised in 2010.

Inci, G. 2008. 3D effects on flood protection levees - Plane strain versus axisymmetric modelling. Proc., 12th Int. Conf. of Int. Association for Computer Methods and Advances in Geomechanics (IACMAG), Curran Associates, Red Hook, NY, 3820-3826.

Low, B.K. 2008. Efficient probabilistic algorithm illustrated for a rock slope. Rock Mechanics and Rock Engineering, Springer-Verlag, Vol. 41, No. 5, 715-734.

Meehan, C. L., and Benjasupattananan, S. 2012. An analytical approach for levee underseepage analysis. Journal of Hydrology. Elsevier, 470-471, 201-211

Meehan, C. L., and Benjasupattananan, S. 2014. An analytical approach for levee underseepage analysis. Journal of Geotechnical and Geoenvironmental Engineering, ASCE, 140(4).

Nanson, Gerald C. 1980. Point bar and floodplain formation of the meandering Beatton River, northeastern British Columbia, Canada. Sedimentology, 27, 3-29.

Nanson, Gerald C. 1981. New evidence of scroll-bar formation on the Beatton River. Sedimentology, 28(6) 889-891.

Petroski, H. 2006. Levees and Other Raised Ground. American Scientist, Vol. 94, No. 1, 7-11.

Polanco, Lourdes and Rice, John. 2014. A Reliability-Based Evaluation of the Effects of Geometry on Levee Underseepage Potential.

Polanco Boulware, Lourdes, "Reliability Underseepage Assessment of Levees Incorporating Geomorphic Features and Length Effects" (2017). All Graduate Theses and Dissertations. 6826.

Rice, John and Polanco, Lourdes. 2012. Reliability-Based Underseepage Analysis in Levees Using a Response Surface–Monte Carlo Simulation Method. Journal of Geotechnical and Geoenvironmental Engineering © ASCE. July 2012.

Saucier, R.T. 1994. Geomorphology and quaternary geologic history of the lower Mississippi Valley. U.S. Army Engineer Waterways Experiment Station, Vicksburg, MS.

Sleep, Matthew, and Duncan, Michael J. 2008. Manual for geotechnical engineering reliability. Report of a study performed by the Virginia Tech Center for Geotechnical Practice and Research. Blacksburg, Virginia. 123 p. 66

SoilVision Systems. 2014. SVFlux. Saskatoon, SK, Canada

Terzaghi, Karl. 1922. Der Grundbruch an Stauwerken and seine Verhiltung (Piping in Dams and Its Prevention). Die Wasserkraft 1724:445-449.

Thorne, C.R., R.D. Hey, and M.D. Newson. 1997. Applied Fluvial Geomorpholgy for River Engineering and Management. John Wiley and Sons, Chichester, UK.

USACE. 2000. Design and Construction of Levees EM 1110-2-1913. Department of the Army, United States Army Corps of Engineers. Washington, District of Columbia.

USACE. 2005. ETL 1110-2-569, Engineering and Design: Design guidance for levee under seepage. Department of the Army, United States Army Corps of Engineers. Washington, District of Columbia.

U.S. Dept. of Agriculture. Soil Conservation Service [USDA SCS]. Soil Survey Staff. 1993, 1983, 1972. Soil Survey Manual. Washington, DC.

William Lettis and Associates, Inc. 2008. Surficial geologic map and initial geomorphic assessment, Sacrament River (east side), Sacramento County, California. Unpublished consultant report prepared for URS Corporation.

Wolff, Thomas F. 2002. ERDC/GSL TR-02-19, Performance of Levee Underseepage Controls: A Critical Review. Department of the Army, United States Army Corps of Engineers. Washington, District of Columbia.

Woolfe, Ken J. and Purdon, Richard G. 1996. Deposits of a rapidly eroding meandering river: terrace cut and fill in the Taupo Volcanic Zone. New Zealand Journal of Geology and Geophysics. 39 (2), 243-249.

Xu B., and Low, B.K. 2006. Probabilistic stability analyses of embankments based on finite-element method. Journal of Geotechnical and Geoenvironmental Engineering, ASCE, 132(11), 1444-1454.

APPENDICES

APPENDIX A

Appendix A presents the families of curves from the response surface developed for straight levee sections, presented in Polanco Boulware (2017). The equation and data tabulated from these families of curves are included in Table A – 1. To use the Response Surface-Monte Carlo method for a point bar in a curved levee section, the user would first calculate the three modified parameters for their levee reach (T_{ch}, RL, and λ_m, discussed in Chapter 4). Using two of these three modified parameters (RL, and λ_m), the user would either select a section in Table A - 1, or interpolate in between sections to determine the values for the constants that need to be substituted into the h_{max} equation provided at the top of the table. Using the constants and the calculated T_{ch} value, the user could then calculate the maximum hydraulic head for a straight levee section, and then apply the curvature multiplier to calculate the maximum hydraulic head for a curved levee section with a point bar.

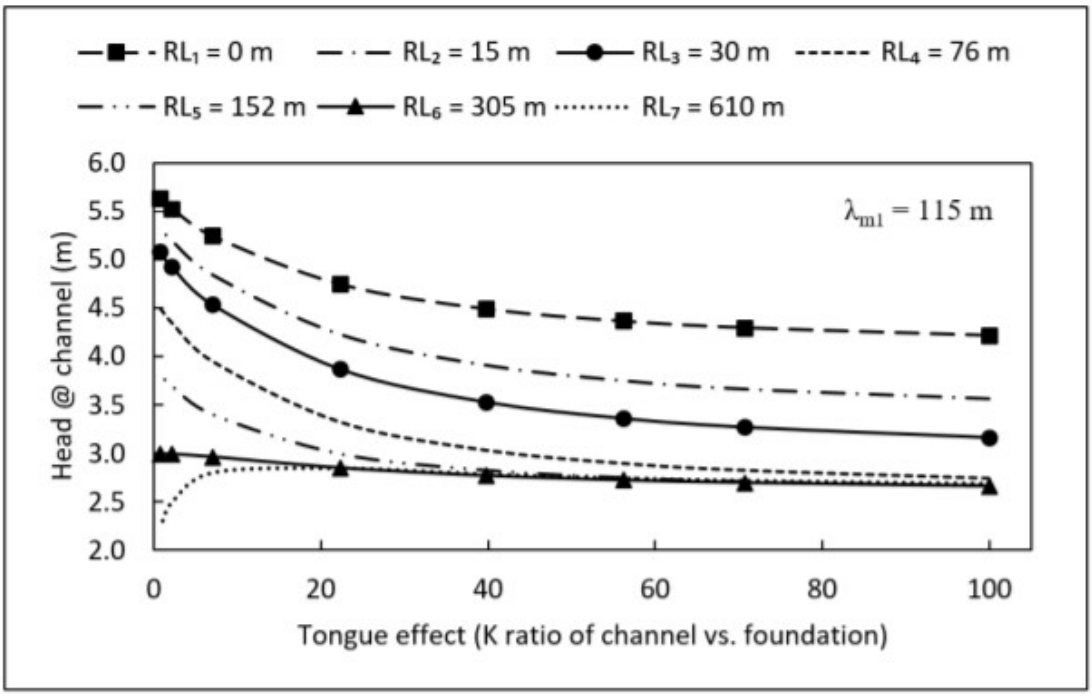

Fig. A - 1. Family of curves for the high conductivity channel model for λm1 = 115 m and different ranges of Tch and RL

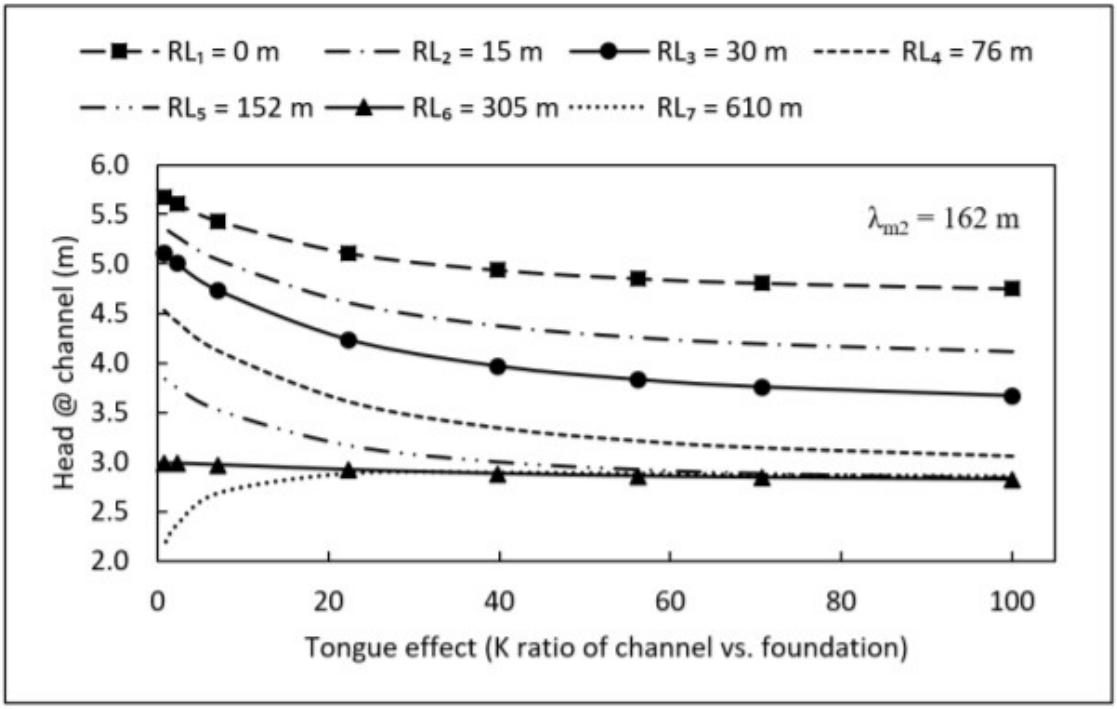

Fig. A - 2. Family of curves for the high conductivity channel model for λm2 = 162 m and different ranges of Tch and RL

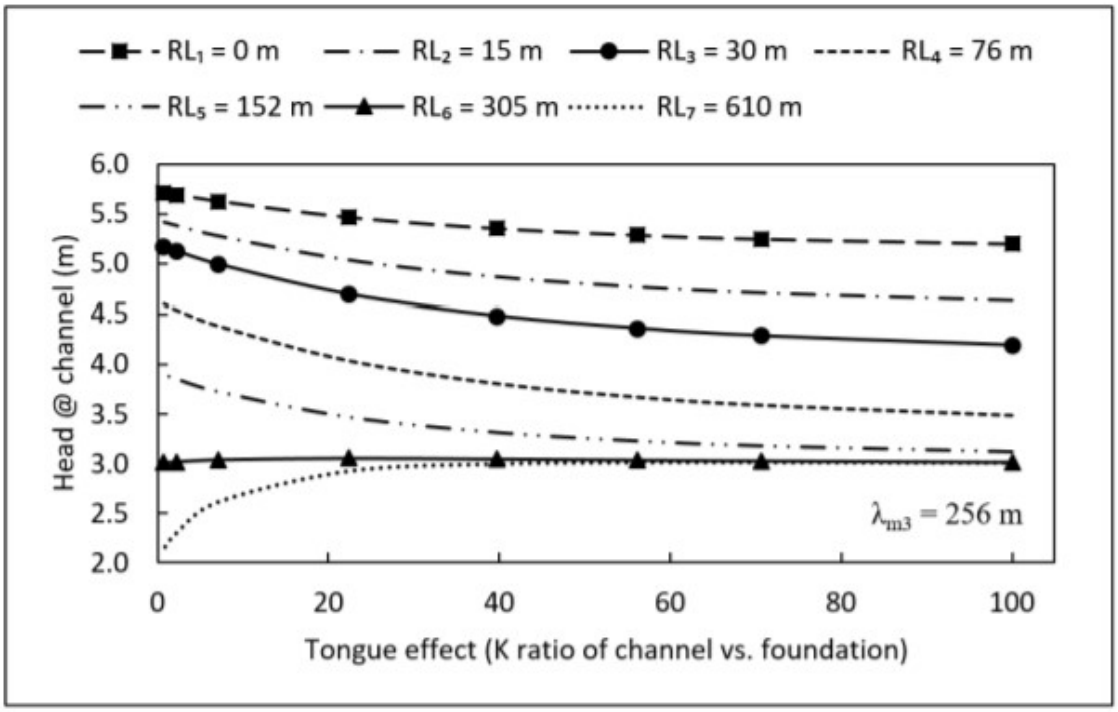

Fig. A - 3. Family of curves for the high conductivity channel model for λm3 = 256 m and different ranges of Tch and RL

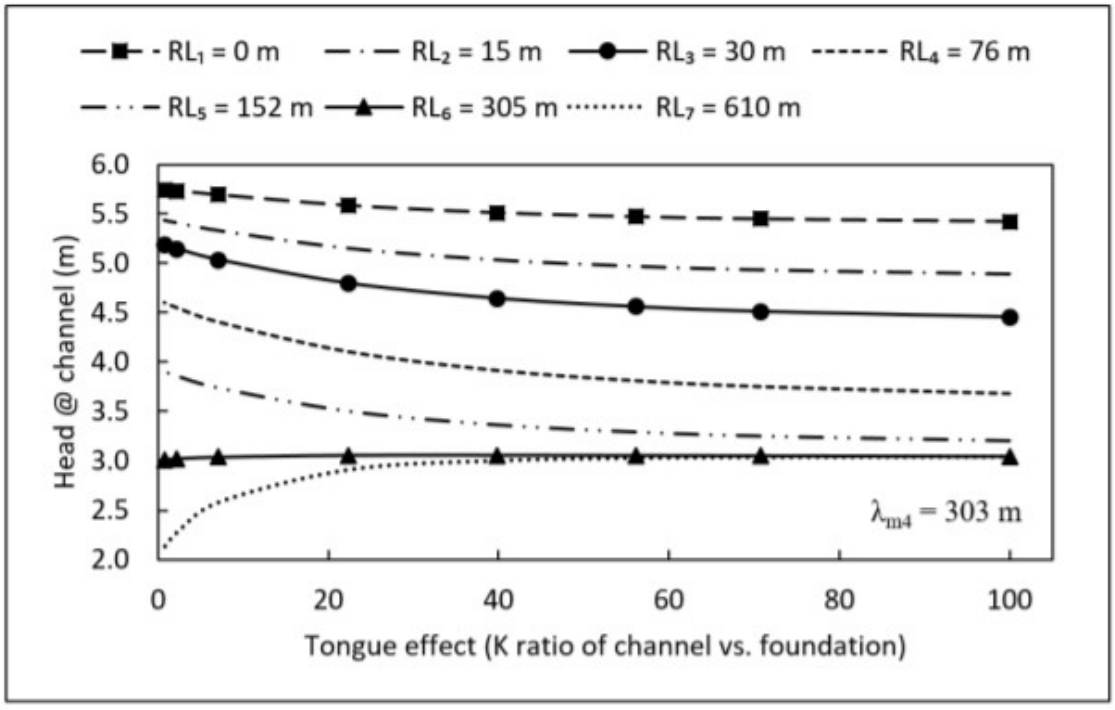

Fig. A - 4. Family of curves for the high conductivity channel model for λm4 = 303 m and different ranges of Tch and RL

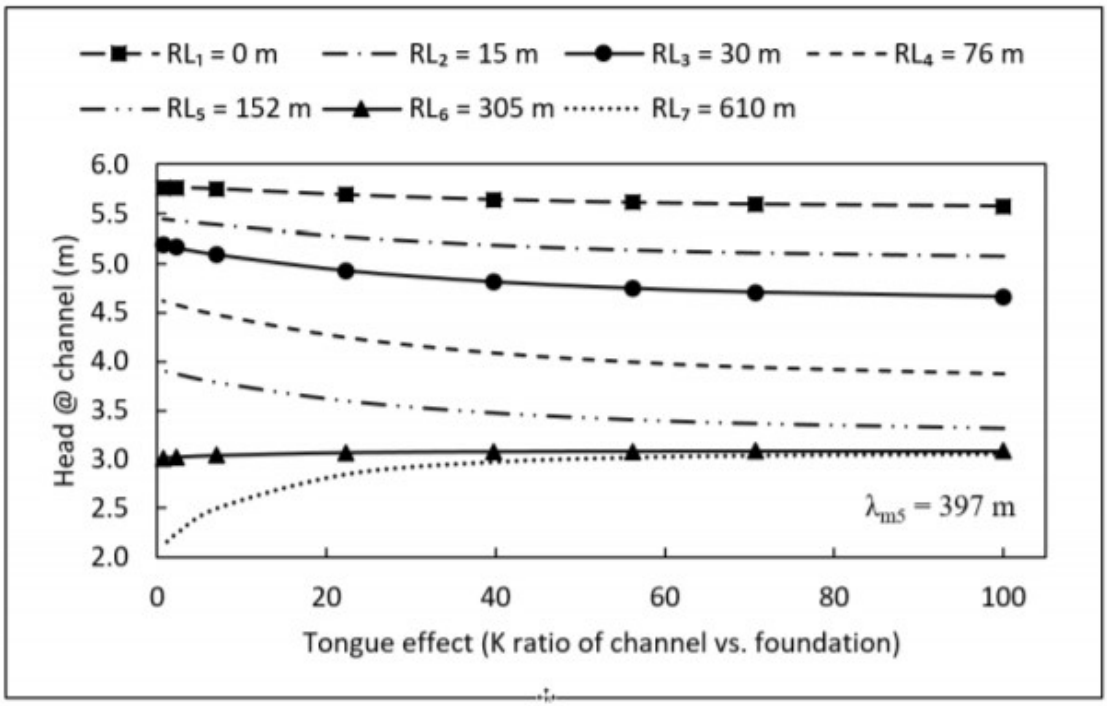

Fig. A - 5. Family of curves for the high conductivity channel model for λm5 = 397 m and different ranges of Tch and RL

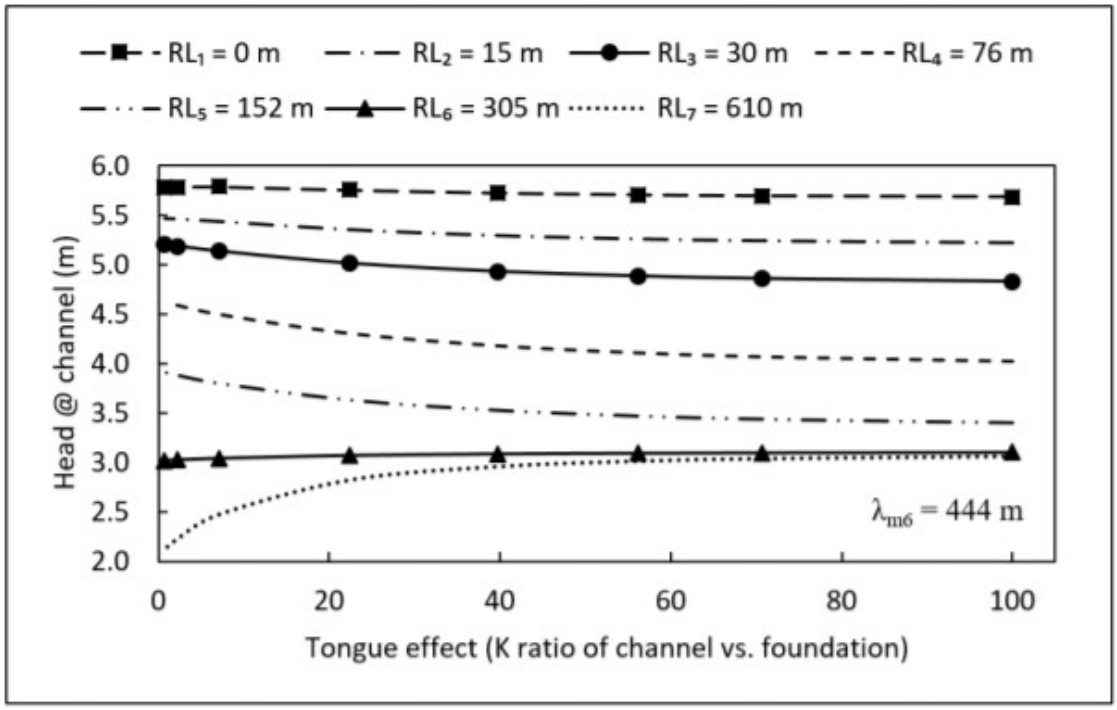

Fig. A - 6. Family of curves for the high conductivity channel model for λm6 = 444 m and different ranges of Tch and RL

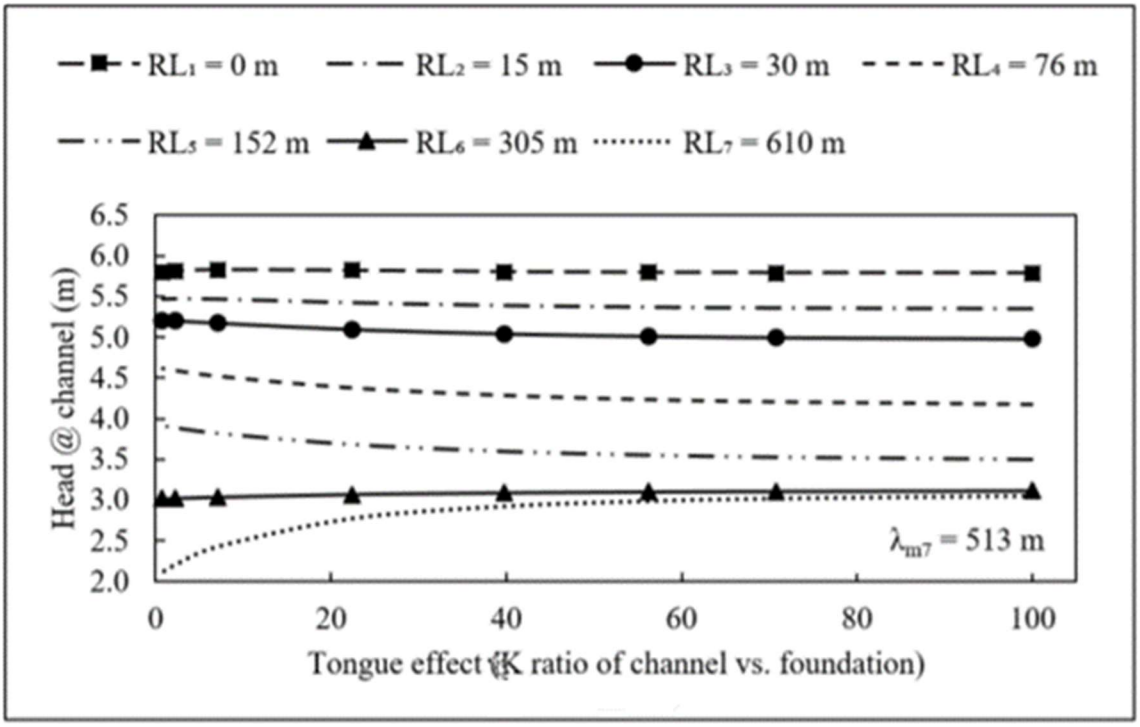

Fig. A - 7. Family of curves for the high conductivity channel model for λm7 = 513 m and different ranges of Tch and RL

Table A - 1. Fit-equations' coefficients and corresponding goodness of fit for family of curves with respect to each λm used

RL (m)	$h_{max} = a_4 * T_{ch}^4 + a_3 * T_{ch}^3 + a_2 * T_{ch}^2 + a_1 * T_{ch}^1 + a_0$						R^2
		a_4	a_3	a_2	a_1	a_0	
Using t_{ch} = 1.5 m and t_b = 0.6 m to compute λ_{m1} = 115 m							
0		6.45E-08	-1.63E-05	1.52E-03	-6.88E-02	5.67E+00	0.99
15		-	-4.47E-06	9.44E-04	-6.75E-02	5.33E+00	0.99
30		-	-4.99E-06	1.05E-03	-7.39E-02	5.07E+00	0.99
76		-	-5.28E-06	1.08E-03	-7.30E-02	4.50E+00	0.99
152		-	-3.99E-06	7.97E-04	-5.13E-02	3.80E+00	0.99
305		-	-2.43E-07	7.49E-05	-8.49E-03	3.01E+00	0.99
610	$T_{ch} \leq 7$	-	-	-1.81E-02	2.30E-01	2.08E+00	0.99
	$T_{ch} \geq 7$	-3.20E-08	7.45E-06	-5.78E-04	1.49E-02	2.72E+00	0.99
Using t_{ch} = 3.0 m and t_b = 0.6 m to compute λ_{m2} = 162 m							
0		3.83E-08	-9.75E-06	9.29E-04	-4.32E-02	5.70E+00	0.99
15		-	-2.98E-06	6.35E-04	-4.64E-02	5.37E+00	0.99
30		-	-3.44E-06	7.33E-04	-5.35E-02	5.12E+00	0.99
76		-	-3.81E-06	8.00E-04	-5.68E-02	4.54E+00	0.99
152		-	-3.03E-06	6.19E-04	-4.17E-02	3.84E+00	0.99
305		-	-9.32E-08	3.08E-05	-3.85E-03	2.99E+00	0.99
610	$T_{ch} \leq 7$	-	1.80E-06	-3.46E-04	1.93E-02	2.58E+00	0.94
	$T_{ch} \geq 7$	-	-	-	7.79E-02	2.15E+00	0.97
Using t_{ch} = 1.5 m and t_b = 3.0 m to compute λ_{m3} = 256 m							
0		4.30E-09	-1.47E-06	2.08E-04	-1.57E-02	5.73E+00	0.99
15		-	-9.91E-07	2.43E-04	-2.23E-02	5.43E+00	0.99
30		-	-1.29E-06	3.10E-04	-2.81E-02	5.18E+00	0.99
76		-	-1.61E-06	3.78E-04	-3.30E-02	4.61E+00	0.99
152		-	-1.44E-06	3.21E-04	-2.56E-02	3.90E+00	0.99
305		-	3.78E-07	-6.86E-05	3.09E-03	3.01E+00	0.99
610		-1.24E-07	2.86E-05	-2.30E-03	7.59E-02	2.13E+00	0.99

Table A-1 (cont'd.)

Using t_{ch} = 3.0 m and t_b = 2.1 m to compute λ_{m4} = 303 m						
0	3.00E-10	-4.65E-07	1.07E-04	-9.66E-03	5.75E+00	0.99
15	-	-8.29E-07	1.98E-04	-1.71E-02	5.45E+00	0.99
30	-	-1.20E-06	2.79E-04	-2.32E-02	5.20E+00	0.99
76	-	-1.60E-06	3.65E-04	-2.99E-02	4.62E+00	0.99
152	-	-1.41E-06	3.10E-04	-2.40E-02	3.91E+00	0.99
305	-	2.84E-07	-5.41E-05	2.88E-03	3.02E+00	0.97
610	-	4.30E-06	-8.24E-04	4.82E-02	2.18E+00	0.97
Using t_{ch} = 3.0 m and t_b = 3.7 m to compute λ_{m5} = 397 m						
0	-6.20E-09	1.17E-06	-4.77E-05	-2.72E-03	5.76E+00	0.99
15	-	-3.72E-07	1.00E-04	-1.01E-02	5.45E+00	0.99
30	-	-6.87E-07	1.69E-04	-1.54E-02	5.20E+00	0.99
76	-	-1.04E-06	2.49E-04	-2.21E-02	4.62E+00	0.99
152	-	-9.53E-07	2.20E-04	-1.85E-02	3.91E+00	0.99
305	-	2.55E-07	-5.21E-05	3.35E-03	3.01E+00	0.99
610	-8.54E-08	2.04E-05	-1.73E-03	6.42E-02	2.09E+00	0.99
Using t_{ch} = 4.6 m and t_b = 3.0 m to compute λ_{m6} = 444 m						
0	-9.80E-09	2.03E-06	-1.23E-04	8.61E-04	5.78E+00	0.99
15	-	-1.93E-07	5.89E-05	-6.44E-03	5.47E+00	0.99
30	-	-5.29E-07	1.29E-04	-1.15E-02	5.21E+00	0.99
76	-	-9.64E-07	2.24E-04	-1.89E-02	4.63E+00	0.99
152	-	-9.03E-07	2.06E-04	-1.67E-02	3.92E+00	0.99
305	-	2.00E-07	-4.33E-05	3.17E-03	3.02E+00	0.99
610	-7.51E-08	1.81E-05	-1.57E-03	6.02E-02	2.09E+00	0.99
Using t_{ch} = 6.1 m and t_b = 3.0 m to compute λ_{m7} = 513 m						
0	-1.30E-08	2.81E-06	-1.94E-04	4.11E-03	5.81E+00	0.90
15	-	2.65E-08	1.02E-05	-2.56E-03	5.48E+00	0.99
30	-	-2.79E-07	7.27E-05	-6.86E-03	5.22E+00	0.99
76	-	-7.60E-07	1.76E-04	-1.45E-02	4.63E+00	0.99
152	-	-7.63E-07	1.73E-04	-1.39E-02	3.92E+00	0.99
305	-	1.61E-07	-3.73E-05	3.10E-03	3.01E+00	0.99
610	-6.10E-08	1.50E-05	-1.33E-03	5.43E-02	2.08E+00	0.99

APPENDIX B

Appendix B presents results from curvature models that were created without point bars. This research was performed for the purpose of comparison with results presented by Benjasupattananan (2013).

Table B - 1. Parameters and normalized results for the curvature model with Dc = 60º and no point bar, to compare with results from Benjasupattananan (2013). ND = arc-length normalized distance from center of curvature. Head measured at landside levee toe and normalized to values calculated on linear sections distant from curved section.

		ND -5	ND -4	ND -3	ND -2	ND -1	ND 0	ND 1	ND 2	ND 3	ND 4	ND 5
Blanket Hydraulic Conductivity (m/s)	Foundation Hydraulic Conductivity (m/s)	Normalized Head (m)										
1E-06	1E-03	1.00	1.01	1.03	1.09	1.24	1.32	1.24	1.09	1.03	1.01	1.00
1E-07	1E-03	1.00	1.02	1.04	1.11	1.25	1.33	1.25	1.11	1.04	1.02	1.00
1E-08	1E-03	1.00	1.02	1.04	1.11	1.25	1.34	1.25	1.11	1.04	1.02	1.00
1E-06	1E-04	1.00	1.00	1.01	1.04	1.18	1.26	1.18	1.04	1.01	1.00	1.00
1E-07	1E-04	1.00	1.01	1.03	1.09	1.24	1.32	1.24	1.09	1.03	1.01	1.00
1E-08	1E-04	1.00	1.02	1.04	1.11	1.25	1.33	1.25	1.11	1.04	1.02	1.00
1E-06	1E-05	1.00	1.01	0.99	1.03	1.19	1.22	1.19	1.03	0.99	1.01	1.00
1E-07	1E-05	1.00	1.00	1.01	1.04	1.18	1.26	1.18	1.04	1.01	1.00	1.00
1E-08	1E-05	1.00	1.01	1.03	1.09	1.24	1.32	1.24	1.09	1.03	1.01	1.00

Table B - 2. Parameters and results for the curvature model with Dc = 90º and no point bar, to compare with results from Benjasupattananan (2013). ND = arc-length normalized distance from center of curvature. Head measured at landside levee toe and normalized to values calculated on linear sections distant from curved section.

		ND -5	ND -4	ND -3	ND -2	ND -1	ND 0	ND 1	ND 2	ND 3	ND 4	ND 5
Blanket Hydraulic Conductivity (m/s)	Foundation Hydraulic Conductivity (m/s)	Normalized Head (m)										
1E-06	1E-03	1.00	1.00	1.02	1.07	1.28	1.42	1.28	1.07	1.02	1.00	1.00
1E-07	1E-03	1.00	1.00	1.02	1.08	1.30	1.44	1.30	1.08	1.02	1.00	1.00
1E-08	1E-03	1.00	1.00	1.02	1.08	1.30	1.45	1.30	1.08	1.02	1.00	1.00
1E-06	1E-04	1.00	1.00	1.01	1.03	1.21	1.33	1.21	1.03	1.01	1.00	1.00
1E-07	1E-04	1.00	1.00	1.02	1.07	1.28	1.42	1.28	1.07	1.02	1.00	1.00
1E-08	1E-04	1.00	1.00	1.02	1.08	1.30	1.44	1.30	1.08	1.02	1.00	1.00
1E-06	1E-05	1.00	1.05	1.17	1.21	1.46	1.51	1.46	1.21	1.17	1.05	1.00
1E-07	1E-05	1.00	1.00	1.01	1.03	1.22	1.34	1.22	1.03	1.01	1.00	1.00
1E-08	1E-05	1.00	1.00	1.02	1.07	1.28	1.42	1.28	1.07	1.02	1.00	1.00

Table B - 3. Parameters and results for the curvature model with Dc = 150º and no point bar, to compare with results from Benjasupattananan (2013). ND = arc-length normalized distance from center of curvature. Head measured at landside levee toe and normalized to values calculated on linear sections distant from curved section.

		ND -5	ND -4	ND -3	ND -2	ND -1	ND 0	ND 1	ND 2	ND 3	ND 4	ND 5
Blanket Hydraulic Conductivity (m/s)	Foundation Hydraulic Conductivity (m/s)	Normalized Head (m)										
1E-06	1E-03	1.00	1.00	1.00	1.03	1.32	1.55	1.32	1.03	1.00	1.00	1.00
1E-07	1E-03	1.00	1.00	1.00	1.04	1.35	1.59	1.35	1.04	1.00	1.00	1.00
1E-08	1E-03	1.00	1.00	1.00	1.04	1.35	1.59	1.35	1.04	1.00	1.00	1.00
1E-06	1E-04	1.00	1.00	1.00	1.00	1.21	1.40	1.21	1.00	1.00	1.00	1.00
1E-07	1E-04	1.00	1.00	1.00	1.03	1.32	1.55	1.32	1.03	1.00	1.00	1.00
1E-08	1E-04	1.00	1.00	1.00	1.04	1.35	1.59	1.35	1.04	1.00	1.00	1.00
1E-06	1E-05	1.00	1.00	1.00	0.95	1.15	1.35	1.15	0.95	1.00	1.00	1.00
1E-07	1E-05	1.00	1.00	1.00	1.00	1.20	1.39	1.20	1.00	1.00	1.00	1.00
1E-08	1E-05	1.00	1.00	1.00	1.03	1.32	1.55	1.32	1.03	1.00	1.00	1.00